Report No. 488

TREATMENT OF ALGAL TOXINS IN DRINKING WATER WITH UV/CL_2 AND UV/H_2O_2 ADVANCED OXIDATION: TOXICITY OF TRANSFORMATION PRODUCTS AND EFFECT ON DISINFECTION BYPRODUCT FORMATION

By
Olya Keen
Fateme Barancheshme

University of North Carolina at Charlotte
Charlotte, North Carolina

wrri.ncsu.edu
NC WATER RESOURCES RESEARCH INSTITUTE

UNC-WRRI-488

The research on which this report is based was supported by funds provided by the Urban Water Consortium through the North Carolina Water Resources Research Institute.

This report fulfills the requirements for a project completion report of the North Carolina Water Resources Research Institute. The authors are solely responsible for the content and completeness of the report.

WRRI Project No. 19-01-U
September 16, 2020

Treatment of algal toxins in drinking water with UV/Cl_2 and UV/H_2O_2 advanced oxidation: toxicity of transformation products and effect on disinfection byproduct formation

Final Report

Olya Keen, PI, UNC Charlotte
Fateme Barancheshme, Ph.D. student

Abstract:
This project evaluated treatment alternatives for water resources contaminated with algal toxins. An established advanced oxidation process (UV/H_2O_2) was compared with an emerging one (UV/Cl_2) in terms of (a) effectiveness for detoxifying the three most common variants of algal hepatotoxin microcystin (LR, RR and YR), and (b) potential to increase the formation of regulated disinfection byproducts [four trihalomethanes (THMs) and nine haloacetic acids (HAAs)] and an unregulated nitrogenous byproduct (NDMA) due to the interaction of the process with algal organic matter and nitrate in the water. The toxicity of the products was assessed with a protein phosphatase inhibition assay (PP2A). Products were also analyzed with HPLC/MS/MS. Disinfection byproducts were assessed using the corresponding EPA methods (551.1, 552.3 and 521) with any modifications described in the report. The results shown that both methods are effective against the three microcystins; however, microcystin LR is also highly susceptible to reaction with chlorine and UV/Cl_2 offers an additional advantage of direct chlorine reaction. The PP2A assay was not able to conclusively determine whether the transformation products retain any residual hepatotoxicity; however, HPLC/MS/MS analysis indicated that ADDA group of the molecule that is considered to be responsible for microcystin toxicity is a susceptible reaction site in both advanced oxidation and direct chlorination, and the resulting products are likely non-toxin. More work needs to be done to determine it with certainty, which may include conducting PP2A assays in pure water samples to avoid matrix interference with the analysis, or performing ADDA-specific assays (e.g. ELISA). Addition of nitrate or algal DOM to the sample matrix did not significantly affect the formation of THMs and HAAs, with the exception of chloroform. However, the effect on chloroform, while statistically significant, is unlikely to affect the regulatory compliance for utilities. On the other hand, NDMA formation was considerably increased by both nitrate and algal DOM. NDMA remained below 10 ng/L which is set as advisory level in some states in all samples. The amounts of nitrate and algal DOM used in the experiments were on the high end of environmentally relevant range. However, formation of nitrogenous DBPs warrants additional investigation.

Table of Contents

List of Figures

List of Tables

Introduction

Toxic algal blooms are a considerable threat to water resources in North Carolina and across the United States.[1] A recent study focused on surface water specifically in the southeastern US found high levels of microcystin group algal toxins.[2] An earlier national survey of water resources indicated that North Carolina has one of the highest levels of cyanobacteria (algae responsible for toxin release) in its water resources,[1] and many of the NC water sources tested by the national study showed the presence of microcystin group of algal toxins. The study that focused specifically on southeastern water resources detected microcystins in 30% of NC water resources and 39% of water resources across the southeastern US in general (75 water bodies assessed).[2] A higher incidence of algal toxins correlates with agricultural and urban development,[3] both relevant to North Carolina.

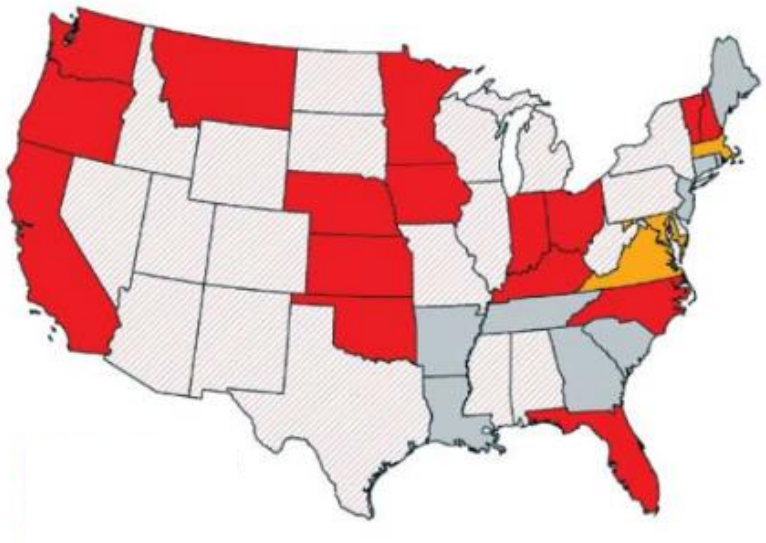

Figure 1. States with reports of cyanotoxin poisoning and health advisories (red) as opposed to only poisonings (orange), only advisories (light gray) or neither (dark gray).[4]

AOPs are currently considered to be one of the best options for managing algal toxins in drinking water treatment.[5] The most common AOP used to treat drinking water combines ultraviolet (UV) and hydrogen peroxide (H_2O_2), although an AOP combining UV and aqueous chlorine (Cl_2) is gaining popularity due to its ease of implementation and operation (it, in essence, adds a chlorine feed to upgraded UV disinfection). UV/H_2O_2, however, is a better understood process with more straightforward chemistry than UV/Cl_2, and the chlorine radicals ($Cl^{\bullet}$) that form during UV/Cl_2 may result in formation of chlorinated organics, many of which can be toxic.

While conventional treatment (coagulation/flocculation, sedimentation and filtration) can effectively remove algal cells, it is ineffective for removal of extracellular toxins already released from the cells.[6,7] Conventional oxidation processes, such as chlorine, chloramine, potassium permanganate and ozone, have a wide range of effectiveness for different toxins across studies, and can release toxins from cells during cell lysis associated with these oxidants.[7,8,9,10,11,12,13] Advanced treatment processes, such as activated carbon adsorption and membrane filtration, can

be effective, but may be cost-prohibitive for some utilities.[7,10,13] Some studies also report selective nature of adsorption for some toxins.[14]

AOPs generate hydroxyl radicals ($HO^{\bullet}$) and sometimes other radical species as well, which react rapidly and non-selectively with a wide range of organic compounds, including algal toxins. In fact, a number of advanced oxidation processes (sonolysis,[15] radiolysis,[16] photocatalysis,[17,18] UV/H_2O_2[19,20]) has been shown to effectively treat various algal toxins.

Despite its relative novelty in water treatment, some utilities are already considering adding UV/Cl_2 capacity to their drinking water treatment train. The UV/H_2O_2 process requires adding more hydrogen peroxide than needed for hydroxyl radical generation due to low UV absorbance of H_2O_2. H_2O_2 residual remaining after the process (typically, 5-10 mg/L) exerts a high chlorine demand (2.09 mg/L of free chlorine per mg/L of H_2O_2), which is costly to the treatment plant. Also, operators who typically lack experience with H_2O_2 and its relatively complex measurement methods can easily misdose the chlorine, leading to a non-optimal chlorine residual in the distribution system. Using UV/Cl_2 avoids this issue because operators are comfortable with measuring and dosing Cl_2. For drinking water treatment plants that use UV for disinfection prior to adding Cl_2 residual for distribution network, process installation can be simply adding a chlorine chemical feed upstream from the UV reactor that is upgraded to deliver a higher UV dose (UV doses required for AOP are approximately 10-50 times higher than those needed for disinfection).

However, little is known about the fundamental chemistry of UV/Cl_2, including the formation of $HO^{\bullet}$ and $Cl^{\bullet}$ and the reaction pathways that determine which products form. Prior studies compared decomposition rates of probe compounds in UV/H_2O_2 and UV/Cl_2 reactions.[21,22,23,24] Some showed that different products form when $Cl^{\bullet}$ is present,[21] suggesting that the reaction with $Cl^{\bullet}$ can be as significant as the $HO^{\bullet}$ reaction in terms of contributing to parent molecule decomposition and determining which products form.

In addition to byproducts of algal toxins, formation of other disinfection byproducts may be affected when advanced oxidation is followed by disinfection. Studies indicate that the presence of algal organic matter in water can lead to higher formation of trihalomethanes (THMs) and haloacetic acids (HAAs).[25,26] Formation of nitrogen-containing DBPs, such as haloacetonitriles, has been documented in the presence of algal organic matter.[27] Other studies show that dissolved organic matter (DOM), in general, can transform during AOP and lead to higher formation of regulated disinfection byproducts,[28] which is of particular concern in the UV/Cl_2 process because of the higher doses of chlorine involved and potential contribution from the reaction between DOM and $Cl^{\bullet}$.

Algal toxins are typically associated with a high nutrient content in source water. In particular, nitrogen has been shown to be the most essential nutrient for toxic algae (with phosphorus being less impactful). In fact, studies show that nitrogen and nitrate are not only predictors of algal blooms, but also of toxin production during the bloom.[29,30,31] Since nitrate (common form of inorganic nitrogen associated with algal blooms) is not removed by conventional drinking water treatment processes, waters containing algal toxins may contain elevated nitrate levels (although nitrate gets taken up by the algal bloom as it progresses). Certain sources of UV used in UV-based AOPs can photochemically activate nitrate, resulting in formation of $HO^{\bullet}$, $NO_2^{\bullet}$ and $NO^{\bullet}$ radicals, as well as other minor radical species.[32,33] These radicals can participate in reactions

with algal toxins and organic matter, and present two concerns: 1) they can generate breakdown products of algal toxins not present in other AOPs that may or may not have additional toxicity; and (2) they can participate in reactions with organic matter and form nitrosamines by providing a reactive nitroso group.

The objective of this project was to determine the conditions (water quality and treatment process settings) under which UV/H_2O_2 and UV/Cl_2 AOPs can be used to treat algal toxins in source water with minimal risks to water utility customers. This objective will be achieved in two tasks:

1) Determine the level of treatment at which UV/H_2O_2 and UV/Cl_2 results in the loss of specific toxicity by common algal hepatotoxins (microcystin variants LR, RR and YR). Assure that no new modes of toxicity (specifically, genotoxicity) form. Determine whether high nitrate affects the toxicity of the products that form due to additional photochemical reactions of nitrate in UV/H_2O_2 and UV/Cl_2 processes
2) Determine how UV/H_2O_2 and UV/Cl_2 treatment of algal organic matter upstream of chlorine disinfection affects formation of disinfection byproducts, including unregulated nitrosamine NDMA (*N*-nitrosodimethylamine).

Materials and Methods

Sample collection and water matrix: The water for use as a background matrix was collected from Mount Holly drinking water treatment plant (DWTP), where no powdered activated carbon (PAC) and preoxidization were utilized (both of which could have altered the nature of the DOM and affected the DBP formation experiments). The water samples were collected in December when no background algal blooms were present. The water volume sufficient for the whole experiment was collected. The water at Mount Holly DWTP goes through coagulation, sedimentation, filtration, and disinfection (chlorine) processes. The water sample was collected before the disinfection unit so that it represents the location where the actual AOP would be placed. Water samples were filtered through 0.45 µm mixed cellulose ester filter that is naturally hydrophilic and has very low extractables, which was experimentally confirmed by running ultrapure water through the filter and measuring TOC/TN content before and after filtration (Appendix A1). Despite low extractables, the filters were prewashed with ultrapure water. The filtered water sample was stored at 4°C for future use. The characteristics of the water sample can be found in Table 1. Nitrate (NO_3-N), nitrite (NO_2-N), ammonia (NH_3-N) and total nitrogen (TN) were measured using Hach Test-in-Tube kits (TNT835, 839, 830 and 10071, respectively). Total Organic Carbon (TOC) was measured using Shimadzu TOC-LCPN instrument using a high temperature combustion method (Standard Method 5310-B). Total organic nitrogen (TON) was calculated as TN minus nitrate, nitrite and ammonia. Total Kjeldahl nitrogen (TKN) was calculated as TON plus ammonia. Bromide (Br^-) was measured using the Dionex ICS-3000 ion chromatography system; Dionex IonPAc AS22 4×250 mm capillary column (Thermo Scientific); Dionex IonPAc AG22 4×50 mm guard column (Thermo Scientific). A solution mixture of 1.7 mM sodium bicarbonate and 1.8 mM carbonate in 18 MΩ·cm ultrapure water served as the eluent. Ultrapure water was used as method blank, and internal and external standards were diluted from purchased standard solution (Sigma-Aldrich).

Table 1. Characteristics of Water Sample

Characteristics	NO_3^--N	NO_2-N	TN	TKN	NH_3-N	TON	TOC	Br^-
Water (mg/L)	0.473	0.013	0.6	0.114	ND	0.114	0.6334	0.105

Algal toxins (Abraxis), nitrate (as $NaNO_3$, Sigma Aldrich) or algal organic matter were added to this matrix as needed to test specific hypotheses. Water matrices for toxicity analysis and DBP analysis are listed in Table 2.

Table 2. Water Matrices

Toxicity Analysis	**DBPs Analysis**
Toxin	Background
Toxin + NO_3^- (20 mg/L as N)	NO_3^-
Toxin + Algal DOM (3 mg/L as C)	Algal DOM
Toxin+ NO_3^-+ Algal DOM	NO_3^-+ Algal DOM

Algal DOM (AOM) extraction: Algal organic matter was generated in the laboratory from *Microcystis sp.* algae (Carolina Biological Supply, Item No. 151840, does not produce toxins) using protocols available in literature.[27] Briefly, *Microcystis sp.* was cultivated at 22°C until the stationary growth phase in 125 mL flasks containing 100 mL BG11 media (Gibco, Thermo Fisher Scientific, US) optimized for the growth and maintenance of Cyanobacteria under a fluorescent lamp with light/dark cycle of 12 h/12 h. BG11 media formulation is included in Appendix A2. New cultures were set up by transferring 5 mL of a stock culture into 100 mL of fresh medium under fluorescent light for ten days to allow the alga to grow. Algal mass was centrifuged at 10,000 rpm for 10 min and
the cells separated during the centrifugation were washed and re-suspended with 100 mL of ultrapure water three times. Next, the cells were subjected to three freeze/thaw cycles at -80°C and 37°C accordingly to lyse the cells. Finally, the solution was filtered through prewashed 0.45 µm cellulose acetate membranes. The organic matter in the filtrate was intracellular organic matter (IOM) which was stored in the dark at -20°C for long term storage and 4°C for short term storage. Figure 2 presents the steps for algal organic matter extraction, and Figure 3 displays the algae culture, cell pellet, and the IOM.

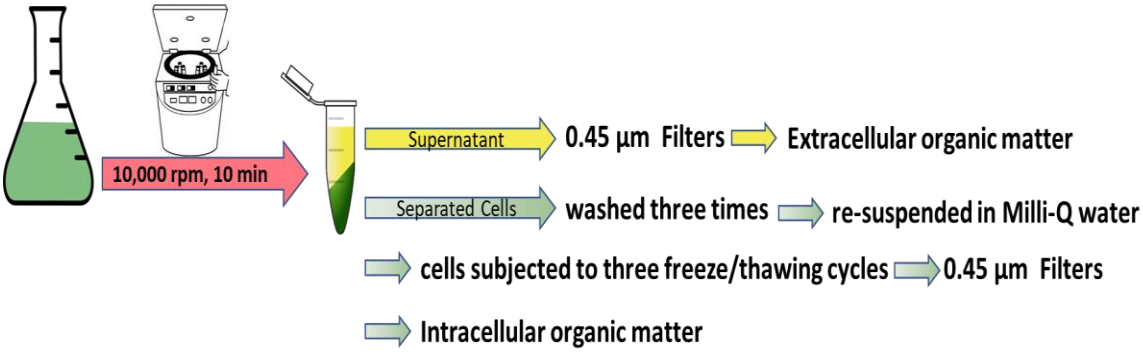

Figure 2. Algal organic matter extraction

Figure 3. (from left) Algae Culture, Cell Pellet, and IOM

Algal organic matter in natural waters experiencing an algal bloom is between 2 and 9.5 mg/L TOC with intracellular organic matter dominating the mix, based on previous studies.[34-36]

The intracellular organic matter was characterized within seven days[36] to determine the carbon and nitrogen content by measuring the following parameters: nitrate (NO_3-N), nitrite (NO_2-N), total nitrogen (TN), total Kjeldahl nitrogen (TKN), ammonia (NH_3-N), total organic nitrogen (TON), and total organic carbon (TOC). The same methods were used as those described for background water characterization. Table 4 includes the characteristics of IOM.

Table 3. Characteristics of IOM

Characteristics	**NO_3-N**	**NO_2-N**	**TN**	**TKN**	**NH_3-N**	**TON**	**TOC**
Concentration (mg/L)	0.328	0.024	14	13.648	0.13	13.518	33.63

Algal toxins: Water samples were spiked with 100 µg/L of MC-LR, 60 µg/L of MC-RR, or 80 µg/L of MC-YR (80, 48 and 64 times the lowest linear calibration standard, respectively). Separate experiments were performed for each toxin. The toxins selected for evaluation were three most common[37] microcystin variants: LR, RR and YR. The spike concentrations were at the high end of environmentally relevant values but within the range of what is detected during toxic algal blooms.[1] MCs standards at 10 µg/mL were obtained from Eurofins Abraxis (Abraxis, PA, USA). Figure 4 shows the chemical structure of target microcystins.

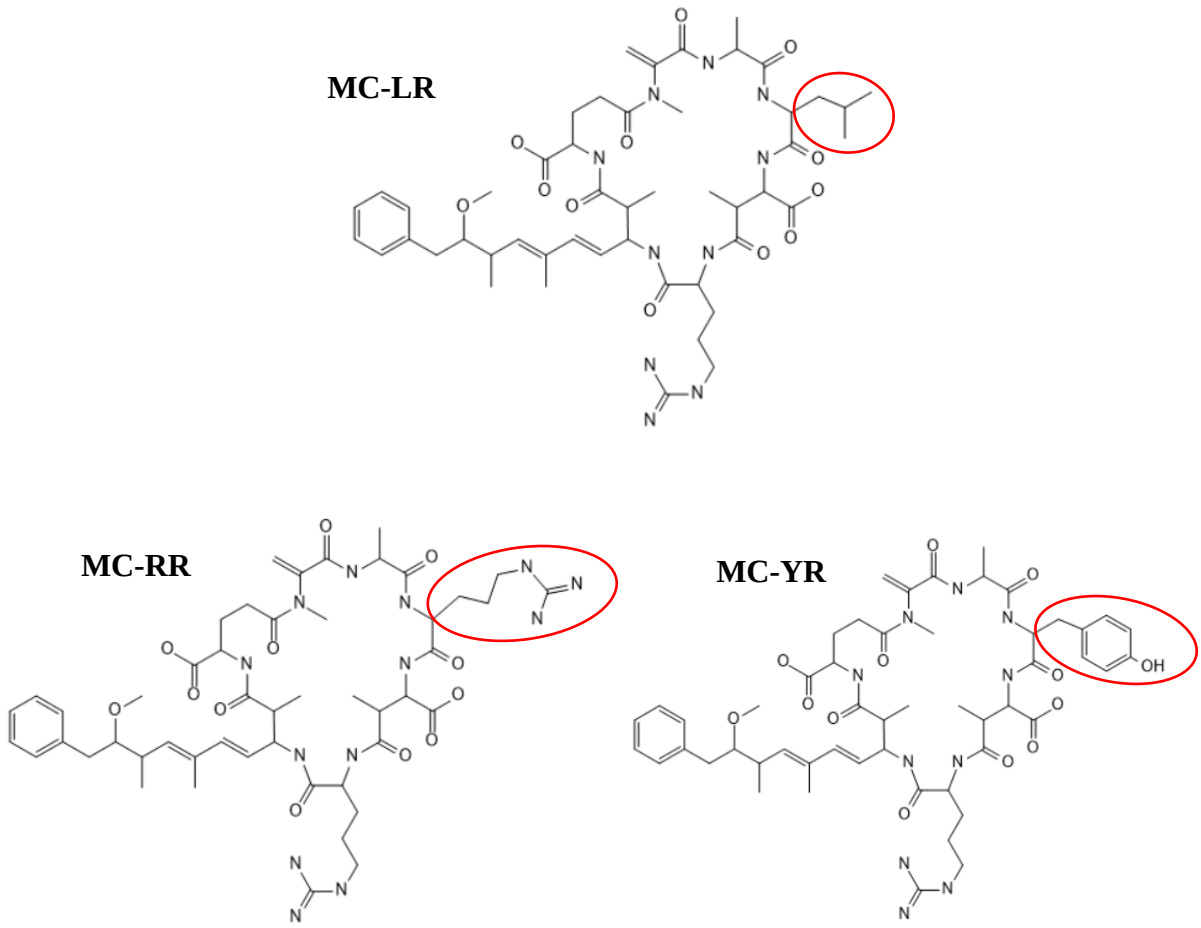

Figure 4. Chemical structure of target microcystins; variable amino acids including tyrosine in MC-YR, arginine in MC-RR, and leucine in MC-LR are circled.

Liquid chromatography and mass spectrometry for microcystin analysis: Samples before and after treatment were analyzed for the concentration of the parent microcystin and any detectable products using liquid chromatography with tandem mass spectrometry system (LC/MS-MS), which consisted of a Thermo Scientific Accela LC and Velos pro-dual-pressure linear ion trap mass spectrometer and a C_{18} column (ZORBAX rapid resolution, Stable Bond, 80Å C18, 3.0 x 100 mm, 3.5 µm, p/n 861954-302). The column temperature was 50°C. Microcystins were evaluated using EPA method 544. Mobile phase consisted of 0.1% formic acid + 5 mM ammonium formate in water (Solvent A) and 80:20 acetonitrile/isopropanol (solvent B). The linear gradient elution condition is shown in Table 4. Before the linear gradient, the first minute of the run at 20% Solvent B was routed to waste to avoid instrument damage from samples and added buffers and quenching agents. After the linear gradient, the column was flushed with 100% Solvent B for 1 minute, then allowed to equilibrate to 20% Solvent B over 5 minutes (Table 4). The solvent flow rate of 0.6 mL/min was used, and the sample injection volume was 10 µL. All solvents were HPLC grade or higher.

Table 4. Linear gradient elution conditions

Time (min)	%B
0	20
4.0	30
6.0	100
9.0	100
10.0	20
15.0	20

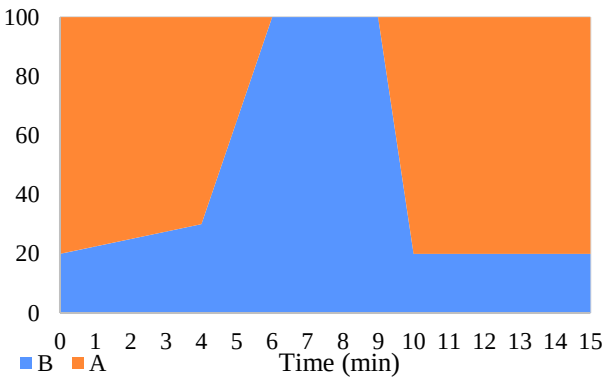

Table 5 presents the molecular formula and molecular weight of MCs. MCs were analyzed using positive electrospray ionization (ESI) MS in full–scan mode to allow the analysis of the degradation byproducts. Table 6 shows the precursor ions and the targeted full-scan MS/MS. The collision energy of 35 eV was provided by nitrogen gas with a flow rate of 0.2 mL/min. The blank and standard solutions containing methanol and MCs stock solution, respectively, were examined using MS analysis with full scan. The standard curves of LC-MS/MS for MCs are displayed in Figure 4.

Table 5. Chemical Properties of MCs

Toxins	CAS no.	Molecular Formula	First Variable Residue (X)	Second Variable Residue (Z)
MC–LR	101043-37-2	$C_{49}H_{74}N_{10}O_{12}$	Leucine	Arginine
MC–RR	111755-37-4	$C_{49}H_{75}N_{13}O_{12}$	Arginine	Arginine
MC–YR	101064-48-6	$C_{52}H_{72}N_{10}O_{13}$	Tyrosine	Arginine

Table 6. MCs Mass Spectrometry Information

Toxins	Precursor Ion	MW (g/mol)	Precursor Ion (m/z)	Targeted Full-Scan (MS/MS)
MC–LR	$[M+H]^+$	994.549	995.6	[m/z 285-1100]
MC–RR	$[M+2H]^{2+}$	1037.566	520.1	[m/z 150-1100]
MC–YR	$[M+H]^+$	1044.528	1045.5	[m/z 285-1100]

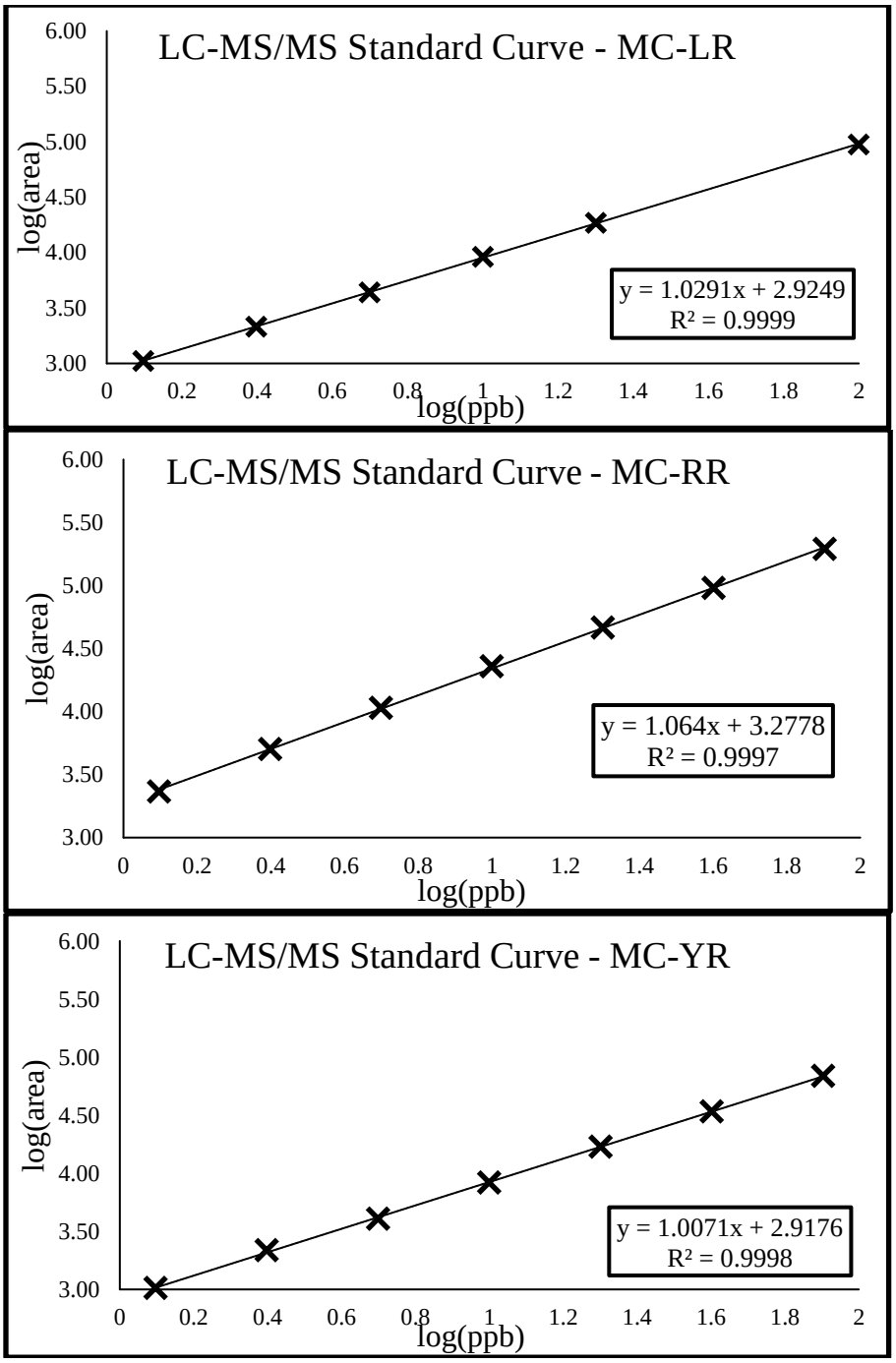

Figure 5. Standard Curves of LC-MS/MS for MCs

AOP experiments: Hydrogen peroxide (H_2O_2) 30% w/w, chlorine 10 to 15% solution of sodium hypochlorite, and ascorbic acid were purchased from Sigma-Aldrich (St. Louis, MO). Ascorbic acid was used to quench Cl_2 and is suitable for the analysis of DBPs.[38] Chlorine was quenched immediately by collecting a sample into a vial containing ascorbic acid at a 150% of stoichiometric concentration to assure that there was no residual chlorine. H_2O_2 was quenched with bovine serum albumin (BSA) (Sigma Aldrich, >96%) which is a suitable quenching agent

for toxicity and LC-MS/MS analysis.[39] The effective concentration of bovine catalase was found based on previous studies[39] and preliminary tests. Bovine catalase of 0.2 mg/L effectively quenched 5 and 10 mg/L of H_2O_2 in less than 10 min with no effect on DBP formation in the uniform formation condition (UFC) test. The concentration of H_2O_2 was measured using triiodide method.[40] For this method, ammonium molybdate, potassium iodide, and potassium hydrogen phthalate were obtained from Sigma-Aldrich (St. Louis, MO). In UV/Cl_2 process, chlorine was measured using *N*, *N*-diethyl-p-phenylenediamine (DPD) Hach powder pillows. Both methods are spectrophotometric, and absorbance was measured using Hach DR6000 UV/Vis spectrophotometer.

AOP experiments were conducted on a bench scale using a quasi-collimated beam apparatus equipped with a 1 kW medium pressure (MP) mercury lamp (Ace Glass). AOP experiments were performed at the ambient pH of the water matrix (6.8). Microcystins have groups that can have both positive and negative charges with pK_A ~2 and the next pK_A ~12.[41] All toxins therefore remained as the same species at the pH used in the experiments as they would be found at the range of environmental water pH (6-9). The UV doses for the MCs AOPs (500-2000 mJ/cm^2) were within the range of full-scale UV doses used in AOPs at drinking water treatment plants. The UV apparatus had two openings for beam collimation; however, the beam is never truly collimated, since some dispersion remains in the beam. Petri Factor was incorporated in the calculations, accounting for the UV irradiance distribution over the sample surface due to the beam dispersion. UV dose determination and bench-scale setup were based on Bolton and Linden's (2003) study (Figure 6).[42] The irradiance for dose determination was measured by a NIST-calibrated radiometer (International Light IL-1400). The spectrum of the medium pressure lamp was measured by a spectral radiometer (Ocean Optics USB2000+). Sample absorbance for UV dose determination was measured by Hach DR6000 spectrophotometer using a quartz cuvette transmitting above 200 nm. Exposure times used to determine the dose were measured by a laboratory timer calibrated against a NIST timer.

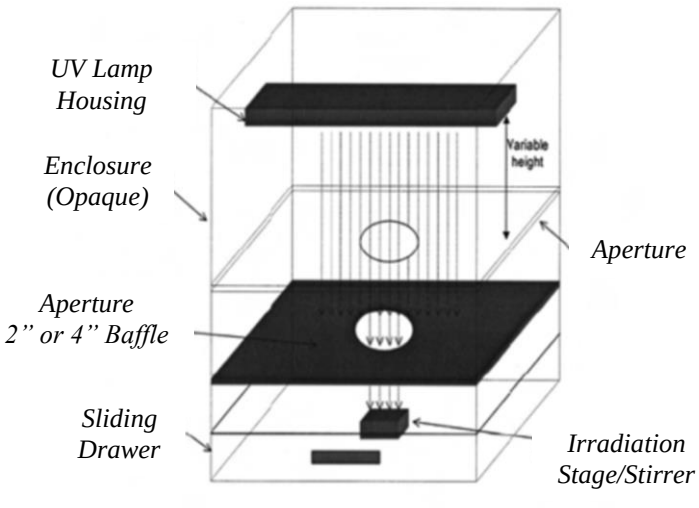

Figure 6. Bench-scale setup for conducting UV experiments.[42]

Figure 7 shows the schematic of experimental matrices. Sixteen different batches were prepared for each of the three toxins which included different matrices and chlorine or hydrogen peroxide

concentrations (with chlorine and hydrogen peroxide added immediately prior to the AOP tests). Each batch was treated under five UV doses (0, 500, 1000, 1500 and 2000 mJ/cm^2) and all experiments were performed in triplicate to determine the statistical significance of the results. Each sample was analyzed for toxin removal using LC-MS/MS and for hepatotoxicity using assays described in the subsequent sections. In addition, 16 batches including different water matrices and chlorine, or hydrogen peroxide concentration were treated under three UV doses (500, 1000 and 2000 mJ/cm^2) for DBPs analysis. These experiments have been performed in triplicate and three samples were collected for each run for THMs, HAAs, and NDMA analysis.

1	2	3
Water Matrix	**UV-AOPs**	**Analysis**
Toxin	5 mg/L H_2O_2	Toxicity Analysis:
Toxin + NO_3^-	10 mg/L H_2O_2	MCs Removal
Toxin + Algal DOM	2 mg/L Cl_2	Hepatotoxicity
Toxin + NO_3^- + Algal DOM	4 mg/L Cl_2 (5 Doses of UV)	Transformation Products
Background	5 mg/L H_2O_2	DBP Analysis:
20 mg-N/L NO_3^-	10 mg/L H_2O_2	Haloacetic Acids (HAAs)
3 mg-C/L Algal DOM	2 mg/L Cl_2	Trihalomethanes (THMs)
NO_3^- + Algal DOM	4 mg/L Cl_2 (3 Doses of UV)	N-Nitrosodimethylamine (NDMA)

Figure 7. Schematic of the experimental matrix

Preliminary testing was performed with each toxin to assure it is non-reactive with H_2O_2. For UV/Cl_2 AOP, due to the reactive nature of chlorine with microcystins, it was dosed into the sample and mixed vigorously immediately before UV exposure. The time in the UV reactor (up to 17 min to achieve 2000 mJ/cm^2 fluence) reflected the residence time of a full-scale process (typically on the order of minutes). At each sampling point, chlorine was quenched immediately by collecting a sample into a vial containing ascorbic acid at a 150% of stoichiometric concentration to quench the amount of chlorine added initially. The excess quenching agent assured that there was no residual chlorine.

Toxicity assays: The hepatotoxicity of treated and untreated samples was determined using protein phosphatase (PP2A) inhibition assay.[43] Figure 8 shows the workflow of PP2A assay. The buffer solution contained the assay components except the fluorescent substrate (Table 7). The buffer and the fluorescent substrate solution (1.7 mM of 4-methylumbelliferyl phosphate) were pre-warmed to 37 $^\circ$C. The clear, flat-bottom, sterile 96-wells plates (200 µL wells) (Qiagen) were prepared by adding 70 µL of buffer solution and 10 µL of different samples including treated sample, untreated sample and background water matix. Then 120 µL of the fluorescent substrate solution was added to all wells simultaneously using an Eppendorf EpMotion96 liquid transfer system. The kinetics and endpoints were read after 1 h using Tecan Genios microplate reader with a fluorescence detector at 360 nm excitation and 465 nm emission. Negative control was a sample with no toxin, and growth kinetics in control wells was considered as 100% enzyme activity reference.

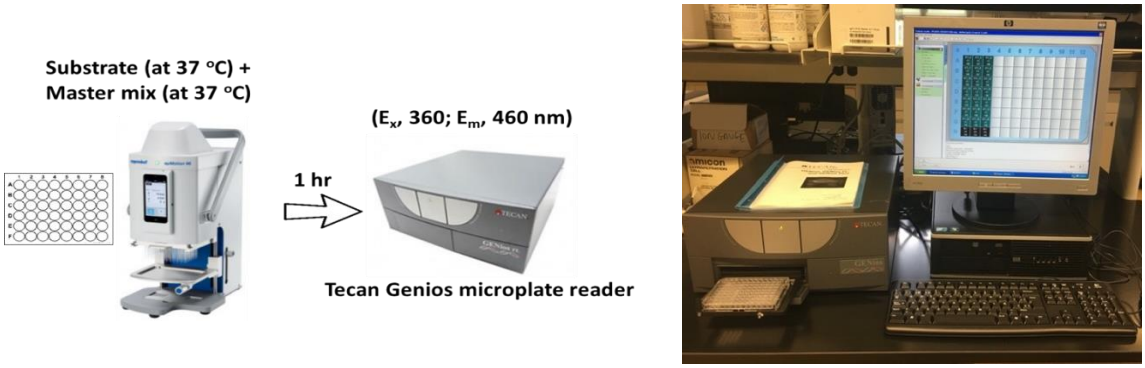

Figure 8. PP2A test workflow

Table 7. PP2A assay mixture

Components	**Amount**
50 mM Tris buffer (pH 7.0) and 0.1 mM $CaCl_2$	50 µL
Enzyme (0.02 U/assay, final concentration, 1.5 nM)	10 µL
40 mM $NiCl_2$	5 µL
5 mL of BSA (1 mg /mL of distilled water)	5 µL
Sample (treated, untreated sample or matrix blank)	10 µL
1.7 mM fluorescent substrate	120 µL
Total	**200 µL**

To prepare 0.1 L of Tris buffer (1 M, pH 7.0), first, 80 mL of distilled water was measured in a suitable container. Second, 12.114 g of Tris base was added to the solution. Then the pH was adjusted to 7.0 using HCl. Finally, distilled water was added until the volume was 0.1 L. Figure 8 shows the PP2A standard curves for MC-LR, -RR, and -YR.

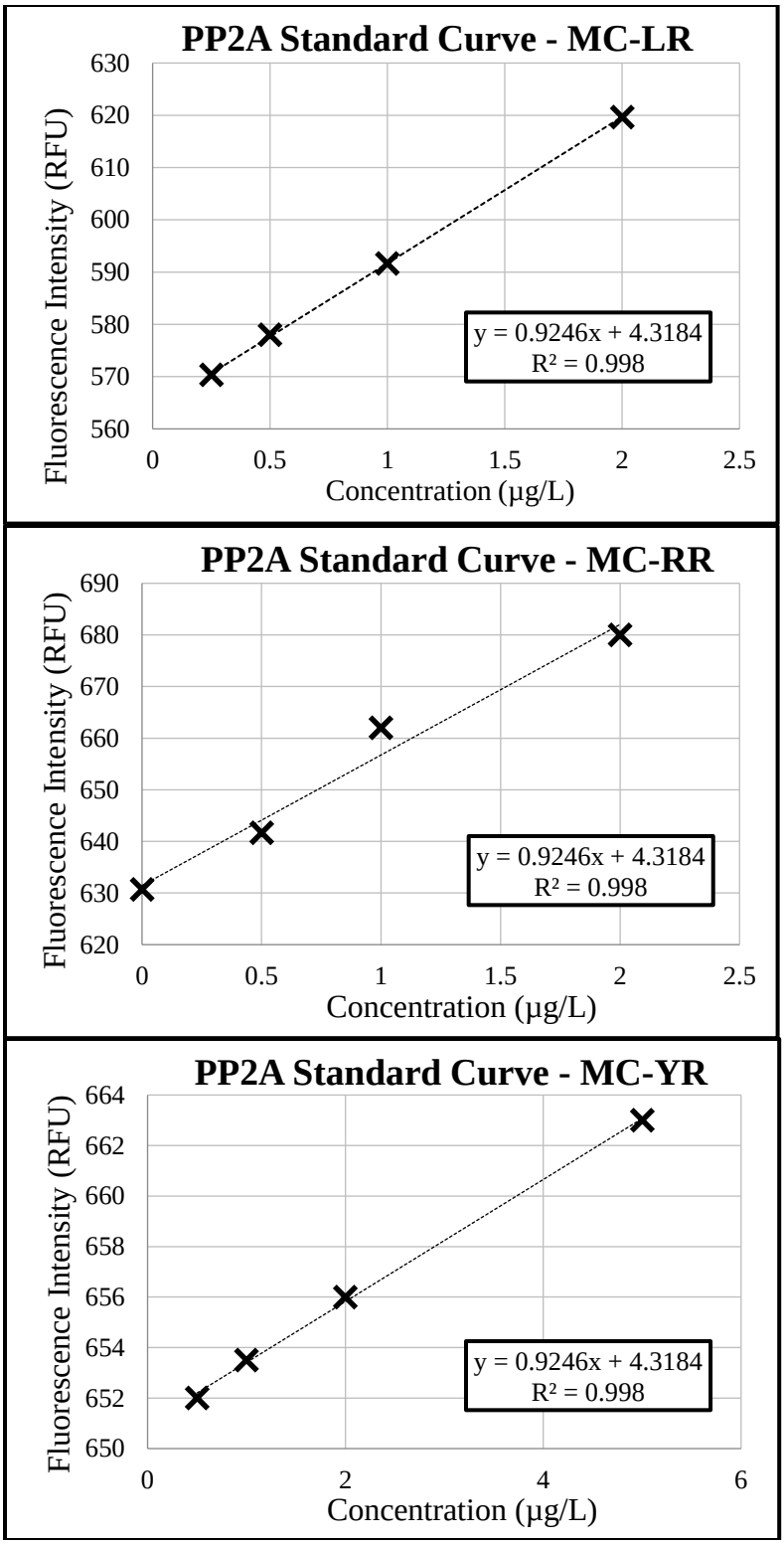

Figure 9. PP2A standard curves for MCs

Disinfection byproduct analysis: Samples were prepared under uniform formation condition (UFC)[44] to analyze disinfection byproducts. Residual chlorine was measured using a Hach DPD powder pillow test that is based on USEPA Method 8167 and 8021 and residual chlorine was quenched using ascorbic acid. Three groups of disinfection byproducts were studied. Four regulated trihalomethanes (THMs) and nine regulated haloacetic acids (HAAs) were analyzed based on EPA methods 551.1 and 552.3 accordingly. These methods were further optimized based on a journal publication.[45] One nitrosamine (*N*–Nitrosodimethylamine, or NDMA) was from the third group of DBPs analyzed and was measured based on a modified EPA method 521 using solid-phase extraction, followed by the LC-MS/MS method developed by Zhao et al. (2006).[46] A six-year review document prepared by the USEPA determined that among different nitrosamines in drinking water, NDMA was being detected most frequently.[47] All of the other nitrosamines were either absent or at very low levels in most of the samples. Therefore, NDMA was selected for this study as a representative nitrosamine.

Uniform Formation Conditions (UFC): Based on the UFC standard operating procedure, each sample was dosed with borate buffer and hypochlorite buffer, and the pH was adjusted to 8.0 ± 0.2. Residual chlorine was 1.0 ± 0.4 mg/L, and the incubation time was 24 h in the dark at 20.0 ± 1.0°C.[44]

A preliminary test was conducted to determine the 24-h chlorine demand of each water matrix and chlorine dose accordingly to achieve 1.0 ± 0.4 mg/L of residual chlorine after 24 h. In this test three chlorine dosages were used based on Cl_2:TOC ratios of 1.2:1, 1.8:1, and 2.5:1. At the end of the chlorine exposure, residual chlorine was measured with Hach DPD test and quenched with ascorbic acid. From the results of these tests, the chlorine dose for UFC was selected to yield a 24-h residual of 1.0 mg/L free chlorine. Cl_2-to-TOC dosage of 2.5:1 worked best with the residual chlorine after 24 h of 0.93 and 1.16 mg/L for water samples with additional algal DOM and water sample without added DOM accordingly. Table 8 shows the results of UFC preliminary dosing tests.

Table 8. Uniform Formation Condition Preliminary Tests

Sample	Cl_2:TOC Ratios	24-h Chlorine mg/L
Matrix without algal DOM	1.2	0.32
	1.8	0.74
	2.5	**1.16**
Matrix with algal DOM	1.2	0.02
	1.8	0.24
	2.5	**0.93**

All bottles and glassware were precleaned using a programmable dishwasher that included the following steps: rinse 3 times with warm tap water, rinse 3 times with deionized water, place in acid bath, rinse with tap water followed by DI water.

Trihalomethanes analysis: THMs were analyzed based on EPA method 551.1. This method was optimized by Liu and their research group.[45] The liquid-liquid extraction method was used to extract the THMs. First, 3.0 mL of methyl tert-butyl ether (MTBE) and 4 g Na_2SO_4 were added to 50 mL of the water sample. Next, the mixture was extracted for 11 min by shaking vigorously. Then, the vial was inverted for five minutes and allowed the water and MTBE phases to separate. After that, 1 mL of the MTBE phase was transferred to an autosampler vial. Finally, 10 µL of 4-bromofluorobenzene as an internal standard was added to the vials, and vials were stored at -20˚C for confirmation analysis.[45]

Gas chromatography with electron capture detector (GC-ECD) was used for THM analysis (Shimadzu-QP2010 GC, Shimadzu, Japan). The instrument was equipped with a split/splitless injector and an electron capture detector (ECD, ^{63}Ni). The analysis was done using splitless mode with the injector temperature at 230˚C. Helium and nitrogen were used as the carrier and makeup gas at a flow rate of 1.4 mL/min and 30 mL/min, respectively. THMs were separated on fused silica DB-1301 capillary column (30 m length, 0.25 mm inner diameter, and 1 µm film thickness with a temperature range between -20˚C and 280-300˚C) (Agilent Technologies, Palo Alto, CA, USA). The oven temperature was maintained at 35˚C for 15 min, and then programmed at 25˚C/min to 145˚C and held for 3 min, and finally 35˚C/min to 240˚C which was held for 5 min. The temperature of the detector was held at 260˚C.

The concentration of THM4 standard solution (Cat. No. 30036 - Restek, PA, US) was 200 µg/mL for each THM. The linearity range of the GC-ECD analysis was 0.01–100 µg/L for THM4. Table 9 shows four THMs targeted in this study. Figure 10 shows the standard curve of each THM compound.

Table 9. THM4 in Standard Solution

Compound	Compound abv	CAS	Concentration	RT (min)
Bromodichloromethane	BDCM	(75-27-4)	200 µg/mL	11.54
Bromoform	BF	(75-25-2)	200 µg/mL	22.44
Chloroform	CF	(67-66-3)	200 µg/mL	28.63
Dibromochloromethane	DBCM	(124-48-1)	200 µg/mL	31.38

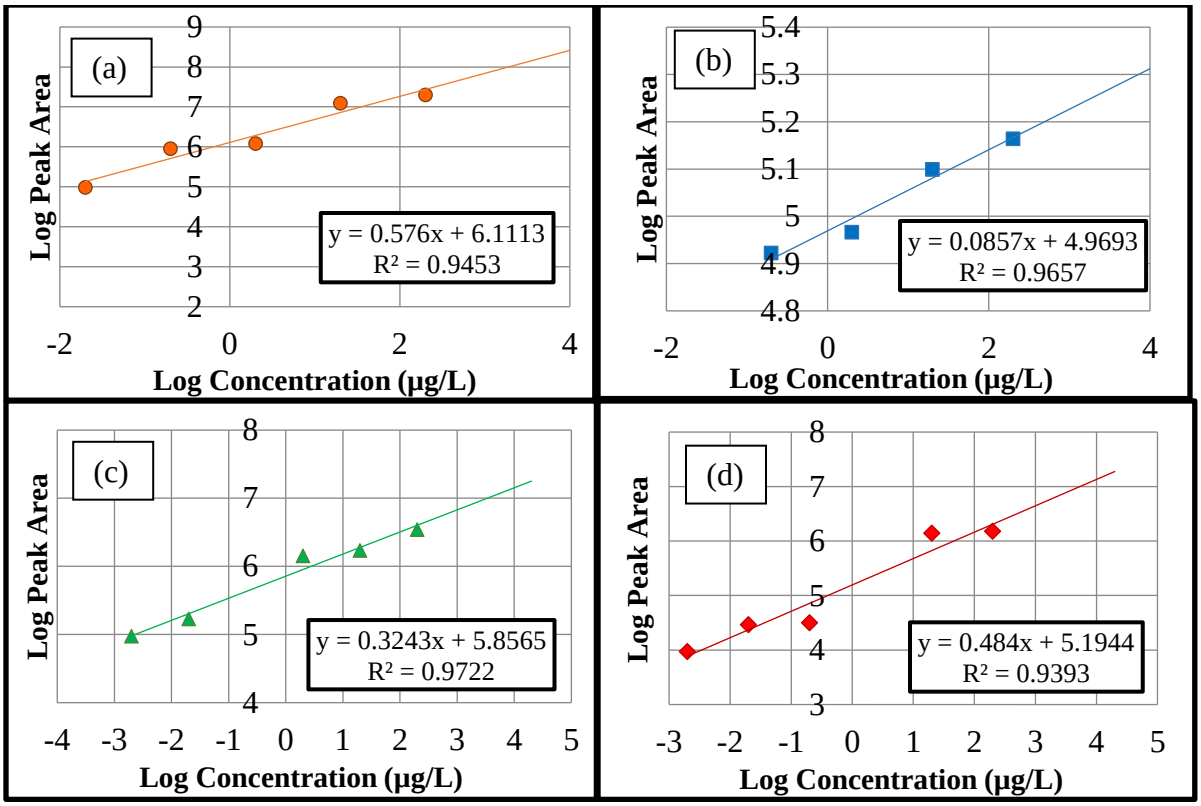

Figure 10. GC-ECD Standard curves of THMs: (a) chloroform, (b) bromodichloromethane, (c) dibromochloromethane, and (d) bromoform

Haloacetic acids analysis: HAAs were analyzed based on EPA method 552.3. This method was optimized by Liu and their research group.[45] The liquid-liquid extraction method was used to extract HAAs. First, 40 mL of the water sample was transferred to a precleaned 60-mL glass vial with a PTFE-lined screw cap using a clean, graduated cylinder for each sample. Next, 2 mL concentrated sulfuric acid (97% ACS grade), and 16 g of Na_2SO_4 was added to the water sample, and the water sample was shaken vigorously by hand until all Na_2SO_4 was dissolved. Next, 3.0 mL of MTBE with internal standard (120 mg/L of 1-2dibromopropane) was added. Next, the sample was shaken vigorously for 14 min, and the phases were allowed to separate for 5 mins. Then 2 mL of the upper MTBE layer was transferred to a 15 mL graduated conical centrifuge tube, and 1 mL of 15% acidic methanol was added to each tube. To prepare 15% acidic methanol, 5 mL of 97% sulfuric acid was added to 60 mL of methanol contained in a 100 mL volumetric flask that was placed in a cooling bath. The solution was mixed and diluted to 100 mL with methanol. Sealed tubes containing sample extract and acidic methanol were placed in a water bath at 40°C and heated for 160 min. Then the tubes were removed from the water bath and cooled to room temperature. After that, 8.5 mL of a 129 g/L Na_2SO_4 solution was added to each centrifuge tube, and the lower layer was discarded. Finally, 1 mL of saturated $NaHCO_3$ solution was added, and the upper ether layer was transferred to an autosampler vial and was stored at -20°C for confirmation analysis.[45] To prepare saturated $NaHCO_3$, sodium bicarbonate was added to 100 mL of water and the solution was mixed periodically until a small amount of undissolved sodium bicarbonate remained despite further mixing.

GC-ECD analysis of HAAs was the same as for THMs except as follows. For HAAs analysis, the SH-Rtx-1701 capillary column (30 m length, 0.25 mm inner diameter, and 1 µm film thickness with a temperature range of -20 to 270/280˚C) (Shimadzu, Japan) was used. The oven temperature was maintained at 40˚C for 10 min, and then programmed at 10˚C/min to 85˚C, and finally 30˚C/min to 205˚C which was held for 5 min. HAAs were analyzed by ECD held at 260˚C.

The HAA9 standard solution was purchased from Restek (Cat. No. 31646, PA, US). Table 10 shows nine HAAs that were targeted in this study. The linearity range of GC-ECD analysis was 0.01–150 mg/L for HAA9. Figure 11 shows the standard curve of each THM compound.

Table 10. HAA9 in standard solution

Compound	**Compound abv**	**CAS**	**Concentration**
Bromochloroacetic acid	BCAA	(5589-96-8)	400 µg/mL
Bromodichloroacetic acid	BDCAA	(71133-14-7)	400 µg/mL
Chlorodibromoacetic acid	CDBAA	(5278-95-5)	1000 µg/mL
Dibromoacetic acid	DBAA	(631-64-1)	200 µg/mL
Dichloroacetic acid	DCAA	(79-43-6)	600 µg/mL
Monobromoacetic acid	MBAA	(79-08-3)	400 µg/mL
Monochloroacetic acid	MCAA	(79-11-8)	600 µg/mL
Tribromoacetic acid	TBAA	(75-96-7)	2000 µg/mL
Trichloroacetic acid	TCAA	(76-03-9)	200 µg/mL

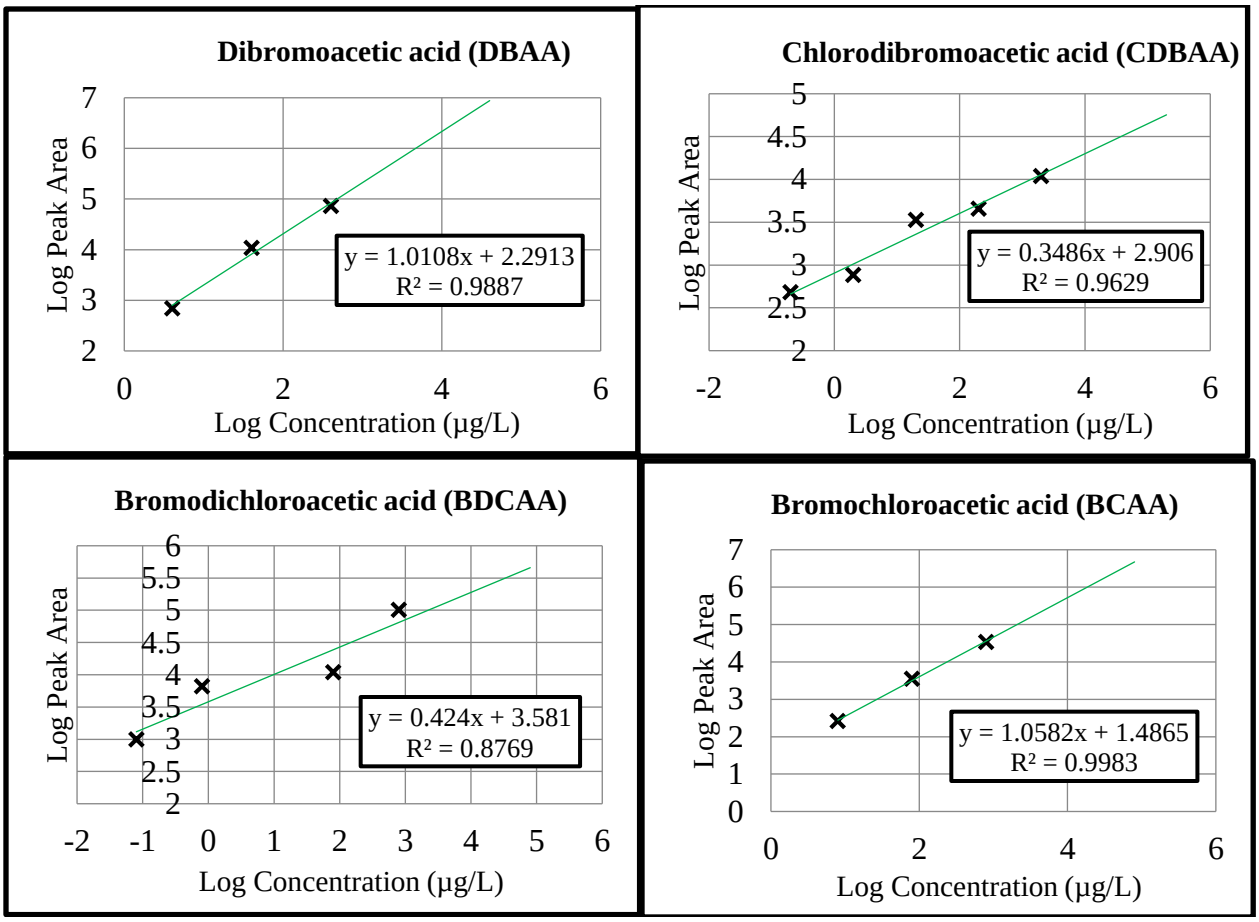

Figure 11. GC-ECD standard curves for HAAs (continued on next page)

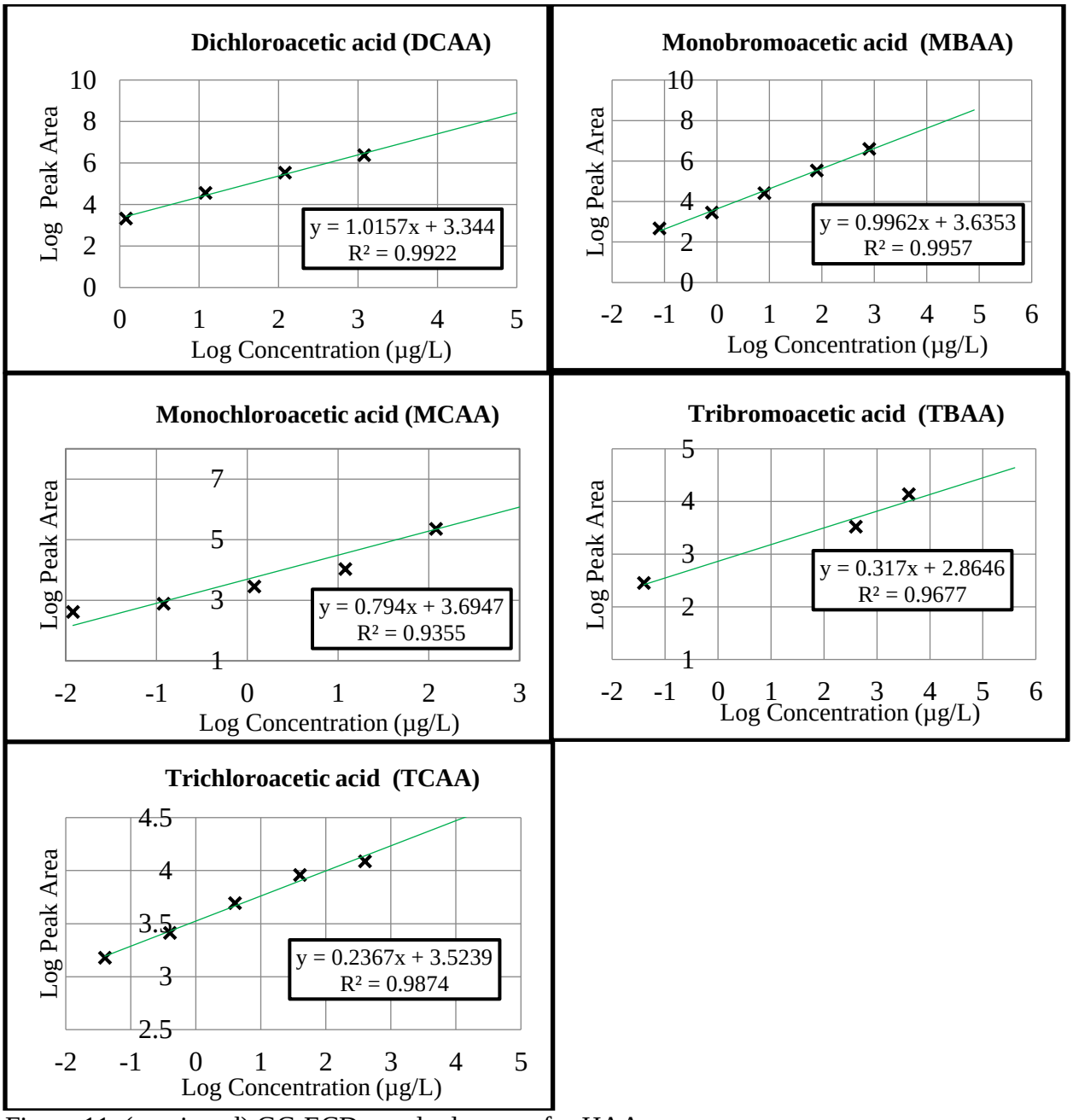

Figure 11. (continued) GC-ECD standard curves for HAAs

Nitrosamines analysis: LC-MS/MS method developed by Zhao et al (2006) was used and included solid-phase extraction (SPE), liquid chromatography (LC) separation, and tandem triple quadrupole mass spectrometry (MS/MS).[46]

The solid-phase extraction (SPE) method using Supelclean™ Coconut Charcoal SPE Tube was utilized to extract the NDMA. The SPE packing material was polypropylene with a bed weight of 2 g and a volume of 6 mL. Charcoal bonding was the active group. The vacuum system (-30 kPa) was used to draw the water sample through the cartridge. The following steps were applied to obtain extracts. First, the SPE cartridges were initially rinsed with 15 mL each of hexane and

dichloromethane, and the residual organic solvents were removed under vacuum. Next, the cartridges were conditioned with 15 mL of methanol and 15 mL of water. Next, 0.5 g of sodium bicarbonate was added to 250 mL of the water sample (pH 8). Then, 25 µL of NDMA-d6 with a concentration of 400 µg/L was spiked into the sample to obtain a final concentration of 40 ng/L. Then, the sample was passed through the SPE cartridge at a flow rate of 3-5 mL/min. After that, the analyte adsorbed on the SPE cartridge was eluted using 15 mL of dichloromethane and was collected in 15 mL tubes and concentrated down to 1 mL under vacuum. Finally, the eluent was transferred to an autosampler vial and was stored at -20°C for confirmation analysis.[48,46] The internal standard NDPA-d14 (100 µL of 200 µg/L) was added to the extract (final concentration of 40 ng/L) before the LC-MS/MS analysis. NDMA-free water was used as a blank and was extracted to ensure all reagents were NDMA-free. A stock solution of 1000 µg/mL and a set of calibration standard solutions of 0.001 to 1000 µg/mL were prepared in methanol and stored in 4ºC. Working solutions of 5 to 200 µg/L in 1:1 methanol/water was freshly prepared before LC-MS/MS. NDMA standard was purchased from Sigma-Aldrich (Cat. No. 48552, Missouri, US).

Agilent 6400 series triple quadrupole LC-MS/MS system was used with positive electrospray ionization combined with the multiple-reaction monitoring (MRM) mode. The mobile phase was 10 mM ammonium acetate and 0.01% acetic acid in water (solvent A) and 100% methanol (solvent B).[46] The solvents were HPLC-grade or higher. The eluent flow rate was 0.3 mL/min. The solvent gradient program included 60% of solvent B for 1 min, then increasing Solvent B to 90% over 5 min and returning back to 60% of solvent B over 0.1 min. Finally, the gradient was returned to the initial conditions by a 3-min re-equilibration before the next sample injection. Injection volume was 100 µL.

The column was a ZORBAX Eclipse XDB-C8 capillary column 4.6×150 mm, 3.5 µm (Agilent Technologies, Palo Alto, CA, USA). MassHunter Quantitation software was used for quantification and the worklist containing all the sample types and calibration level was set up. The peaks of standards and extracted samples were monitored automatically and results were reproducible. MS/MS parameters including collision energy and cell accelerator voltage are shown in Table 11. Gas flow rate was 10 L/min at 350°C.

Table 11. Optimized LC-MS/MS conditions for NDMA detection

Compounds	Parent Ion (m/z) $[M+H]^+$	Product Ion (m/z) $[M+H]^+$	Collision Energy (eV)	Cell Accelerator Voltage
NDMA	75	43	15	4
NDMA-d6	81	46	25	4
NDPA-d14	145	97	25	4

Figure 12 presents the LC-MS/MS calibration curve for NDMA. LC-MS/MS analysis was linear in the whole range of 0.001–1000 µg/L for NDMA.

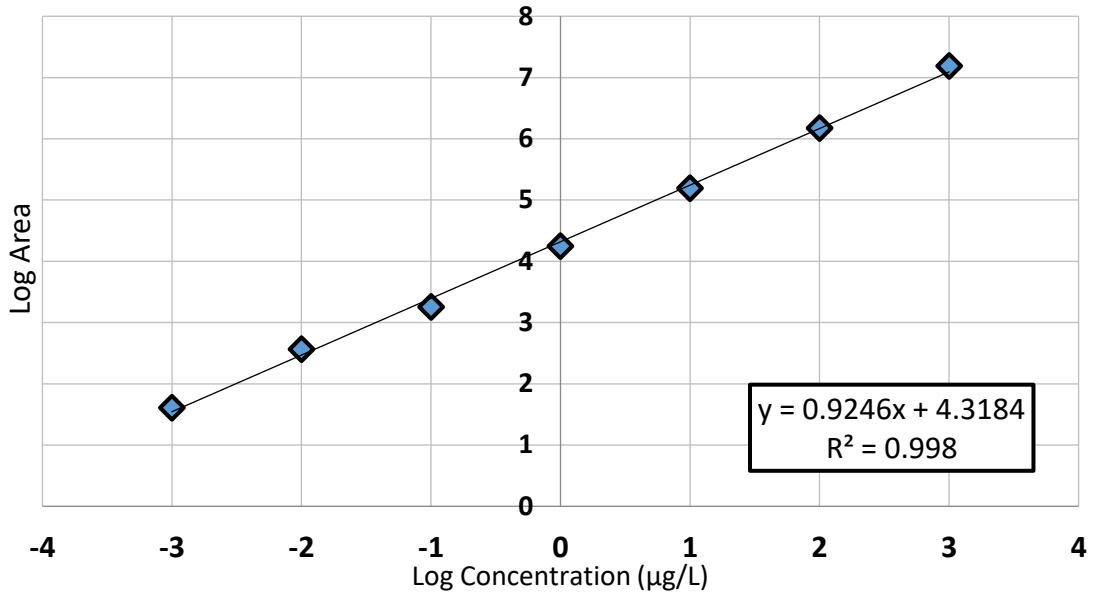

Figure 12. LC-MS/MS Calibration Curve for NDMA

T-test analysis of DBP results: Two-sample t-tests were performed in Excel to evaluate the significance of any differences in samples means of DBP formation between the samples. Null hypothesis is that the means of two group are equal. If the t-statistic value is smaller than -t-critical or higher than +t-critical then the null hypothesis is rejected. Rejecting the null hypothesis means that the results are statistically significantly different, and failing to reject the null hypothesis means that the results are not significantly different. The p-value reflects whether the difference is statistically significant. Smaller the p-values mean that the evidence to reject the null hypothesis is stronger. A p-value less than 0.05 (at 95% confidence level) is statistically significant.

Results

Comparison of UV/H_2O_2 and UV/Cl_2 AOPs for algal toxins treatment: Figures 13 to 15 show the degradation of MCs-LR, -RR, and -YR as a function of UV dose in the presence of 5 and 10 mg/L of H_2O_2 and 2 and 4 mg/L of Cl_2 and different types of water matrices. It is evident from the results that a single process is not a clear best option for all three microcystins. All four processes performed very well for MC-RR achieving upwards of 70-90% decrease in MC-LR concentration at all UV doses tested. At the same time, UV/Cl_2 process was much more efficient for MC-LR because of the fast direct reaction between MC-LR and free chlorine. An opposite was observed for MC-YR which showed better degradation of the parent compound in UV/H_2O_2 process compared to UV/Cl_2. Literature indicates that the three variants tested in this study have similar reactivity with both free chlorine[49,50] and with hydroxyl radicals,[51] which indicated that the contribution from chlorine radicals forming in UV/Cl_2 process may have been the reason for the observed differences. Additionally, while direct UV photolysis is reported to be of little contribution to the overall AOP processes for MC-LR,[51] sufficient information is not available for the other microcystins, especially for the low wavelengths emitted by medium pressure

mercury vapor lamps. Therefore, direct photolysis by UV may have contributed to some of the observed differences in the response from the three microcystin variants tested in this study.

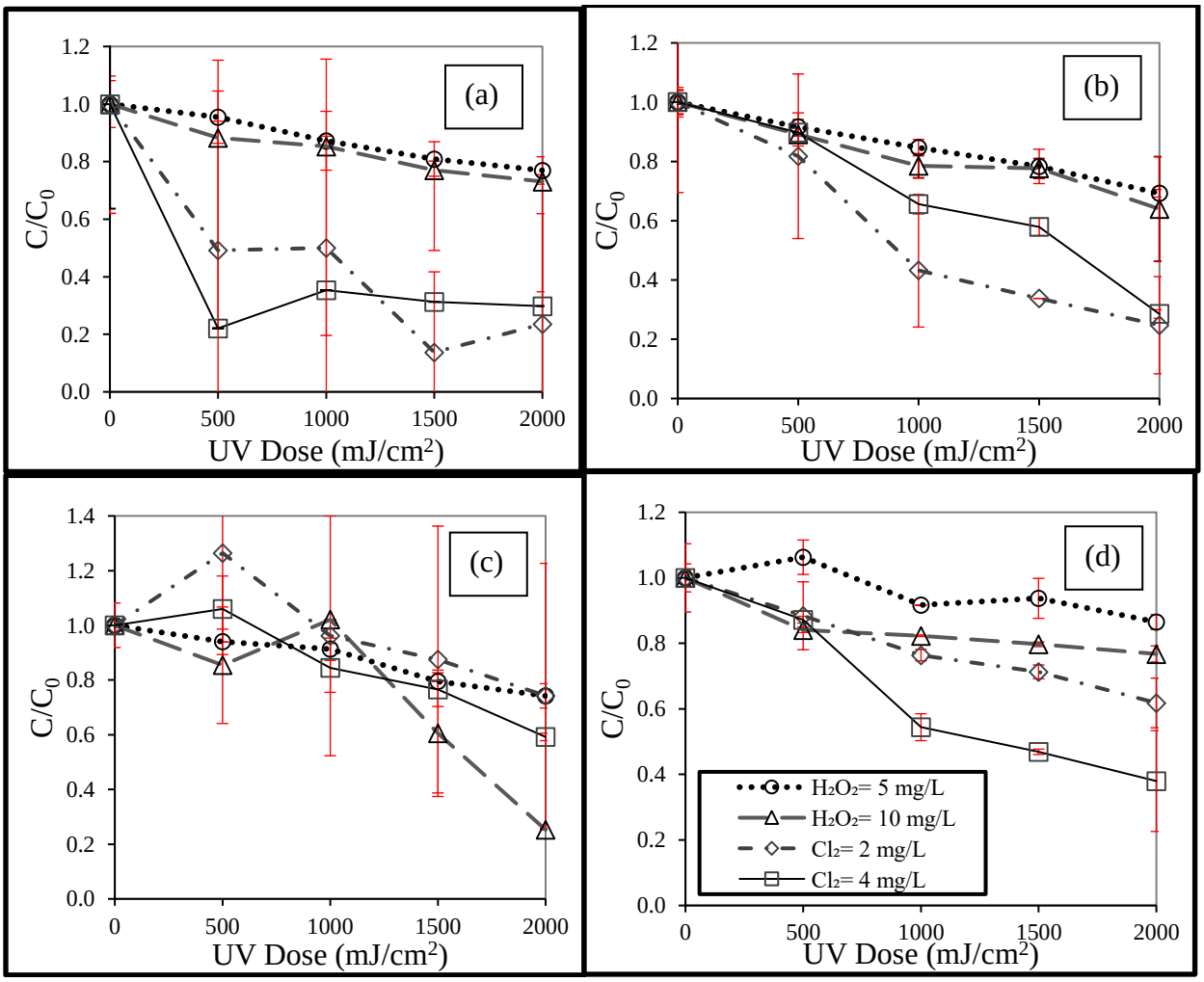

Figure 13. Fraction of MC-LR remaining in tested AOP processes in (a) background matrix; (b) with additional 20 mg-N/L of nitrate; (c) with additional 3 mg-C/L algal DOM; and (d) with both additional nitrate and DOM. Data shows the average of three replicates and the error bars are the standard deviations. The legend is for all four plots.

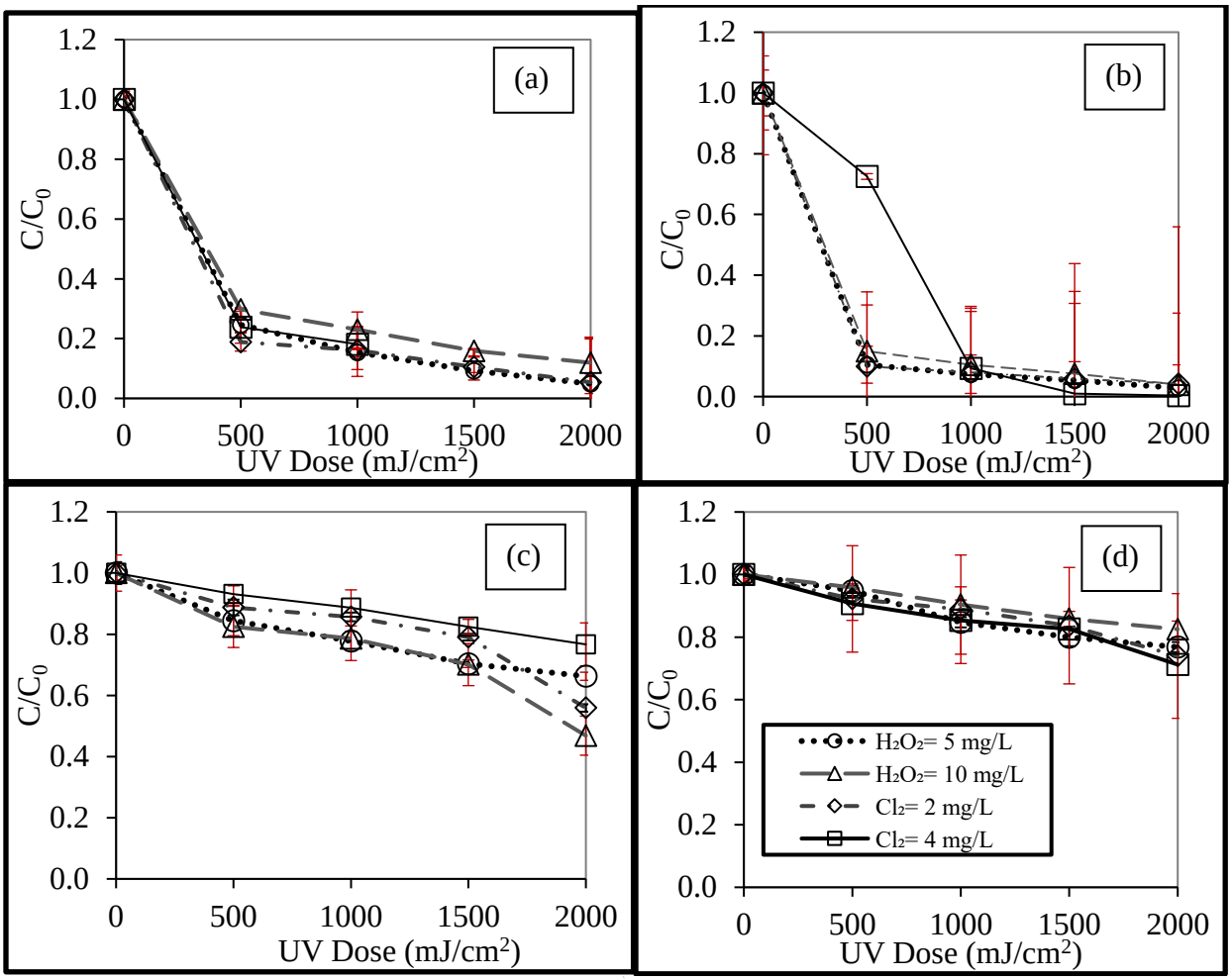

Figure 14. Fraction of MC-RR remaining in tested AOP processes in (a) background matrix; (b) with additional 20 mg-N/L of nitrate; (c) with additional 3 mg-C/L algal DOM; and (d) with both additional nitrate and DOM. Data shows the average of three replicates and the error bars are the standard deviations. The legend is for all four plots.

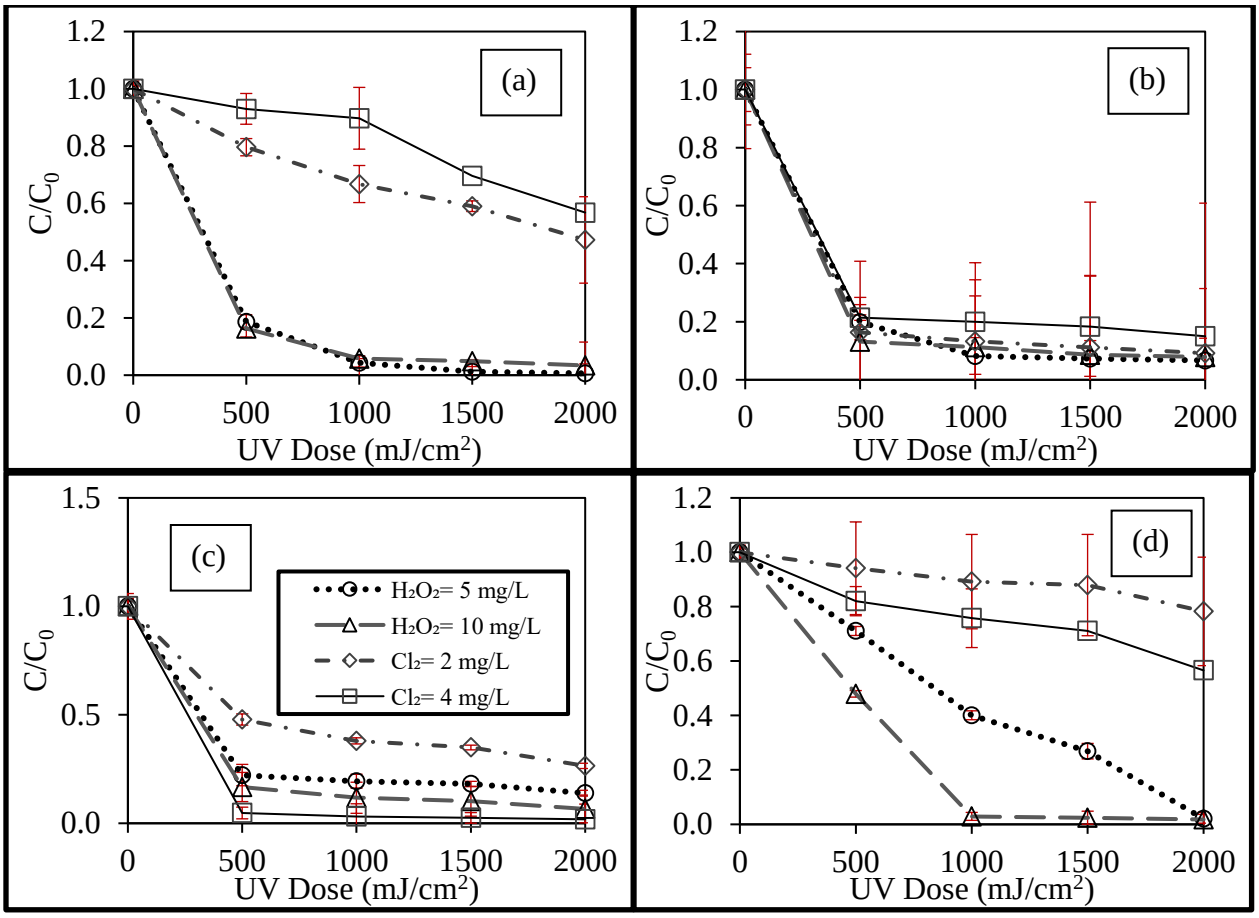

Figure 15. Fraction of MC-YR remaining in tested AOP processes in (a) background matrix; (b) with additional 20 mg-N/L of nitrate; (c) with additional 3 mg-C/L algal DOM; and (d) with both additional nitrate and DOM. Data shows the average of three replicates and the error bars are the standard deviations. The legend is for all four plots.

Matrix effects differed for each microcystin. Table 12 shows the removal efficiency of different treatment methods under 500 and 2000 mJ/cm^2 in various matrices. In general, elevated nitrate resulted in additional hydroxyl radicals[32,33] and resulted in similar performance for the two AOP processes as radical reactions were prevalent over direct reactions with Cl_2. Additional AOM in the matrix not only scavenged the radicals, but it also reacted with Cl_2, which reduced the effectiveness of both processes considerably. The results are consistent with other studies that show that the presence of DOM decreases the removal efficiency in UV/Cl_2 and demonstrate its impact as background scavenger of both radicals and oxidant.[22] The presence of AOM specifically has an even stronger negative effect on the removal rate in AOPs because of the high reactivity of AOM with HO$^{\bullet}$.[36] The second-order rate constants of *Microcystis aeruginosa* extracted AOM (IOM) with HO$^{\bullet}$ was determined as 4.45×10^8 M^{-1}.s^{-1}.[36] However, the reaction rate constant of standard DOM with HO$^{\bullet}$ was reported as 3.6×10^8 M^{-1}.s^{-1} by Westerhoff et al. (1999)[52] showing that the scavenging potential of AOM is higher than DOM standards. The effect of DOM as a hydroxyl radical scavenger was observed for all three MCs. When both AOM and nitrate were present in the matrix, the positive effect of nitrate in generating more hydroxyl radical was suppressed by AOM scavenging of the radicals, especially in UV/H_2O_2 process.

Table 12. Removal efficiency (%) of MC-LR, -RR, -YR UV/H_2O_2 and UV/Cl_2

Matrix	Oxidant Dose	MC-LR		MC-RR		MC-YR	
		UV = 500 mJ/cm^2	UV = 2000 mJ/cm^2	UV = 500 mJ/cm^2	UV = 2000 mJ/cm^2	UV = 500 mJ/cm^2	UV = 2000 mJ/cm^2
Background	H_2O_2 = 5 mg/L	4.56	23.06	75.39	95.12	81.40	99.36
	H_2O_2 = 10 mg/L	11.75	26.92	70.21	88.08	83.65	96.60
	Cl_2 = 2 mg/L	50.79	76.39	81.19	94.60	20.38	52.77
	Cl_2 = 4 mg/L	70.18	77.93	76.19	93.70	7.00	43.21
Nitrate = 20 mg/L	H_2O_2 = 5 mg/L	8.43	30.75	89.49	97.20	80.18	93.33
	H_2O_2 = 10 mg/L	10.84	36.05	85.06	96.08	86.85	92.13
	Cl_2 = 2 mg/L	18.26	75.26	90.08	95.77	83.71	90.83
	Cl_2 = 4 mg/L	10.30	71.48	27.51	99.68	78.58	85.00
DOM = 3 mg/L	H_2O_2 = 5 mg/L	6.02	25.78	15.55	33.75	77.78	86.11
	H_2O_2 = 10 mg/L	14.60	74.74	17.60	53.17	83.28	93.38
	Cl_2 = 2 mg/L	12.51	25.77	11.25	44.11	52.15	73.53
	Cl_2 = 4 mg/L	5.99	40.80	6.90	23.32	95.26	98.17
DOM = 3 mg/L, and Nitrate = 20 mg/L	H_2O_2 = 5 mg/L	6.29	13.48	5.17	23.20	5.87	21.72
	H_2O_2 = 10 mg/L	15.88	23.22	4.17	17.50	17.96	43.41
	Cl_2 = 2 mg/L	11.58	38.18	7.80	26.03	28.92	97.93
	Cl_2 = 4 mg/L	12.78	62.02	9.29	28.79	52.01	98.21

Based on the reaction rate of MC-LR under UV photolysis and with hydroxyl radicals, higher removal efficiency was expected at 2000 mJ/cm^2 in all matrices and treatment conditions. The removal efficiency of MC-RR and -YR under high UV dose were in line with expected values based on reaction rates. Additionally, the results for MC-LR had more scatter in data than the other two toxins. MC-LR samples experienced prolonged storage during laboratory closures to prevent the spread of novel coronavirus. While the samples were stored in a way that is standard for preservation of LC-MS samples (frozen at -20°C), it may have affected their quality.

Therefore, it is reasonable to conclude that both UV/Cl_2 and UV/H_2O_2 AOP will work just as well for MC-LR as they did for the other two MCs.

Hepatotoxicity assay: Cyanotoxins are mainly classified into three groups, including hepatotoxic peptides, neurotoxins, and contact irritants based on their significant toxicological impact.[53] MCs are hepatotoxins and can act as tumor promotors as they can inhibit protein phosphatase enzymes in liver.[53] Figures 16-18 show the measured hepatotoxicity of the water samples using PP2A enzyme inhibition assay after various treatment conditions. As described in the method section, higher concentration of toxins inhibits more PP2A and decreases the fluorescence intensity. Fluorescence intensity indicates the activity of protein phosphatase with fluorescent substrate.[54]

While the results for the most part showed a fluorescence signal unchanged by treatment, it is not because the toxicity of the parent-product mixture is not decreasing with treatment. Instead, if the results of the samples are compared to the standard calibration curves in terms of fluorescence intensity, it is evident that the sample background matrix has a major interfering effect for this assay. The standard calibration curves in ultrapure water matrix had a fluorescence signal on the order of 600-700 relative fluorescence units (RFU), while samples in a natural water matrix had a fluorescence signal on the order of 10,000 (RFU), and increased approximately 4 times after nitrate was spiked in (the response to AOM was less intense). The background components of the water matrix appear to have a fluorescence signal that is many times that of the toxin, and at this level of interference, it cannot be reliably factored out by running appropriate matrix controls. Any incremental change in fluorescence due to changes in the toxin will be not distinguishable within the signal variability from the water matrix. Therefore, LC-MS/MS analysis of transformation products for MCs was performed to assess the potential of the transformation products to have residual toxicity. The results are presented in the next section.

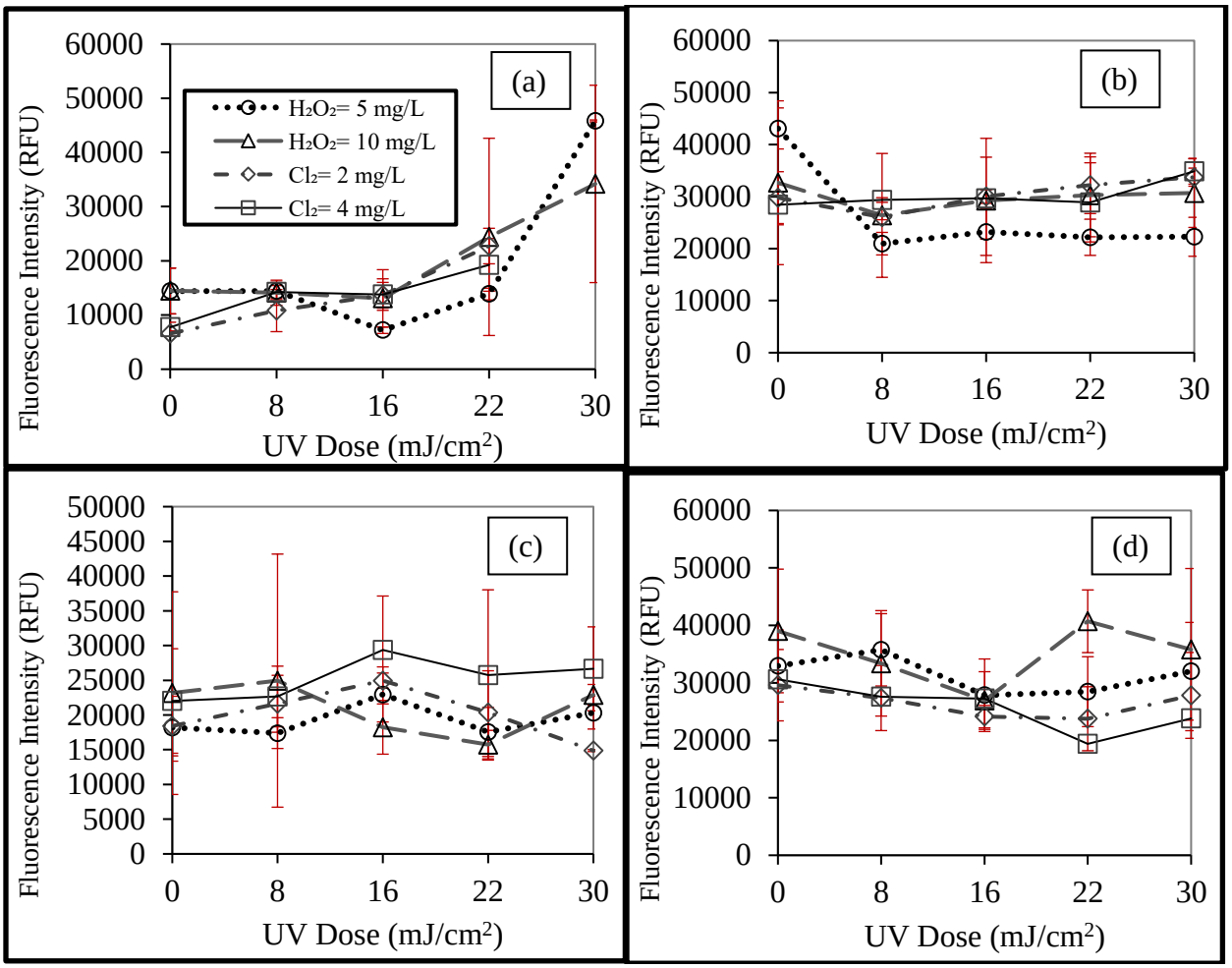

Figure 16. Fluorescence intensity in PP2A assay for MC-LR as a function of treatment in (a) background matrix; (b) with additional 20 mg-N/L of nitrate; (c) with additional 3 mg-C/L algal DOM; and (d) with both additional nitrate and DOM. Data shows the average of three replicates and the error bars are the standard deviations. The legend is for all four plots.

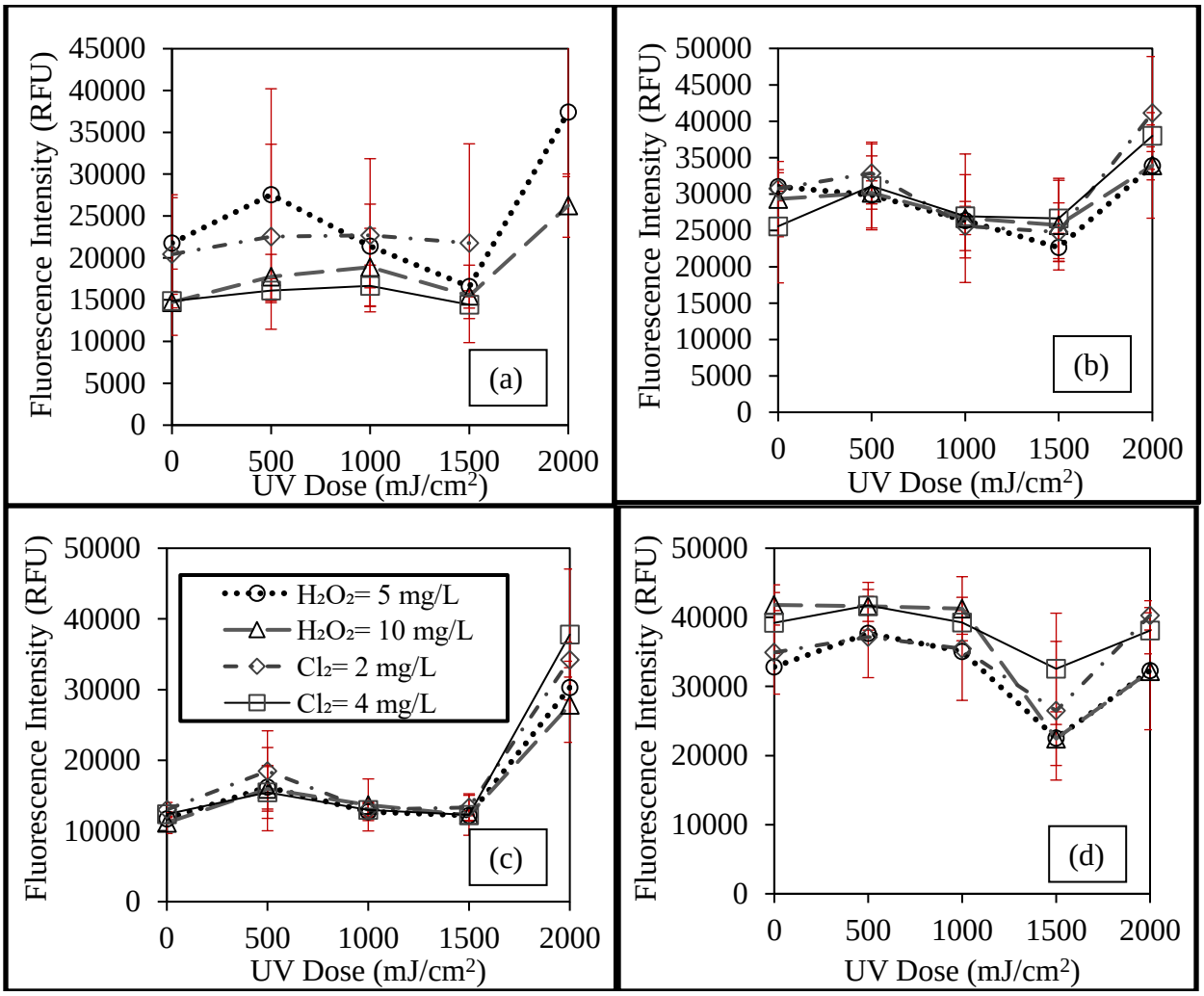

Figure 17. Fluorescence intensity in PP2A assay for MC-RR as a function of treatment in (a) background matrix; (b) with additional 20 mg-N/L of nitrate; (c) with additional 3 mg-C/L algal DOM; and (d) with both additional nitrate and DOM. Data shows the average of three replicates and the error bars are the standard deviations. The legend is for all four plots.

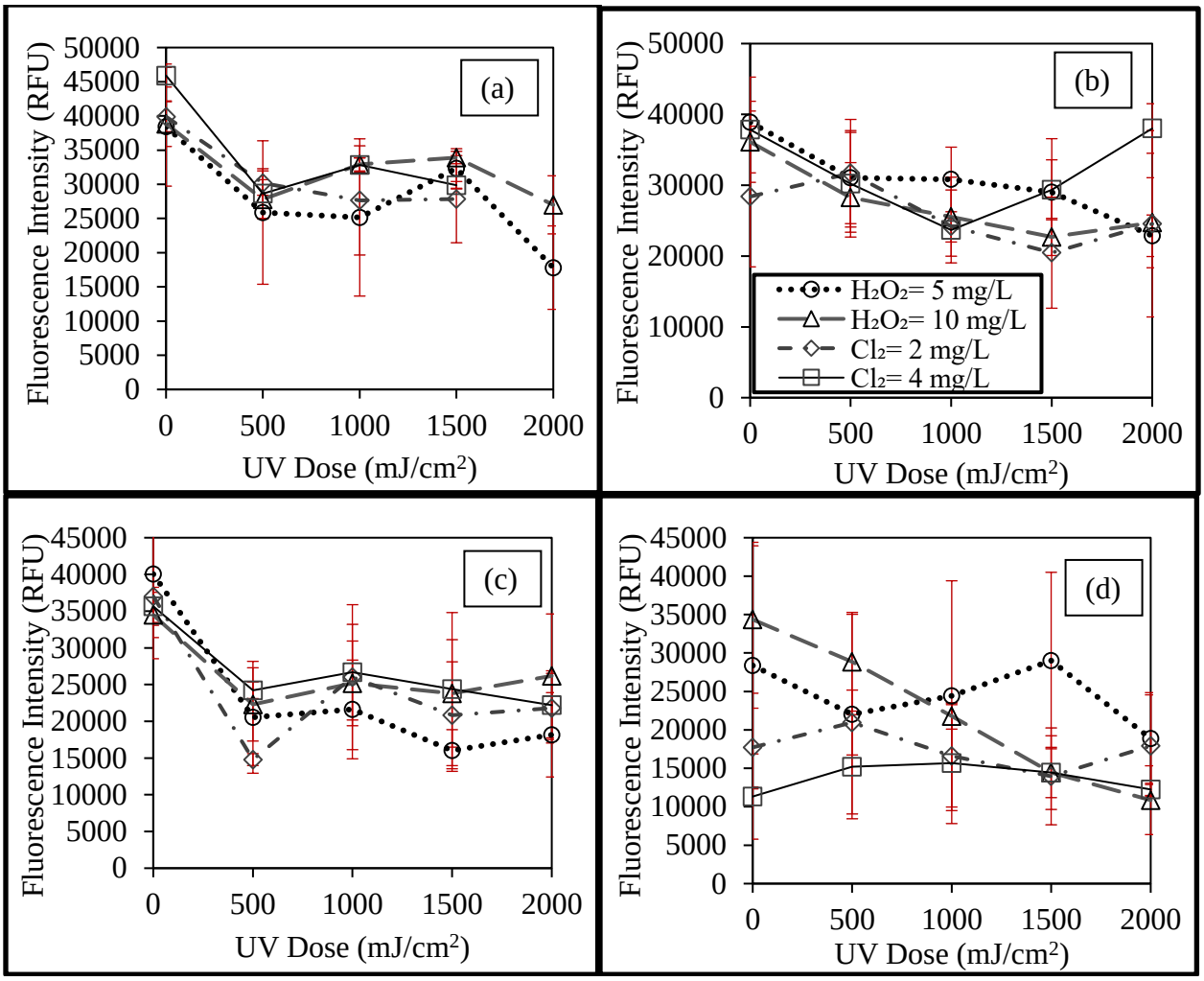

Figure 18. Fluorescence intensity in PP2A assay for MC-YR as a function of treatment in (a) background matrix; (b) with additional 20 mg-N/L of nitrate; (c) with additional 3 mg-C/L algal DOM; and (d) with both additional nitrate and DOM. Data shows the average of three replicates and the error bars are the standard deviations. The legend is for all four plots.

Transformation products: Degradation byproducts were determined using fragmentation results obtained by LC-MS/MS as well as isotope ratios for chlorinated products, and nitrogen rule. Four main products were detected (m/z 732, 748, 790 and 674) in both UV/Cl_2 and UV/H_2O_2. Some of the products were common among mycrocystins. MC-LR had m/z 732 and 748 as major products in UV/H_2O_2. In UV/Cl_2, additional product was observed with m/z 790. MC-YR had products with m/z 732, 790 and 674 in both UV/H_2O_2 and UV/Cl_2 processes. None of the observed products appear to have chlorine addition in their structure (chlorine has a distinct isotope pattern in mass spectrometry). Products of MC-RR could not be analyzed because a different LC-MS method was used (selected ion monitoring rather than full scan). However, based on the similar response of the other two MCs, it is conceivable to conclude that the same groups shared among the MCs will have the vulnerability.

As all of the product m/z values are even numbers and the parent m/z values are odd numbers (m/z 995 for MC-LR and m/z 1045 for MC-YR), nitrogen rule states that an odd number of nitrogen atoms was lost from the molecular structure. Nitrogen atoms that are part of the larger cyclic structure of the molecule are not as accessible to participate in a reaction as external functional groups are, so it is reasonable to assume that the nitrogen loss occurs at the triamine group of the molecule (Reactive Site 1 in Figure 19). Additionally, Adda group (amino-9-methoxy-2,6,8-trimethyl-10-phenyl-4,6- decadienoic acid) loss is likely, based on the molecular weight of the products, which makes it a second vulnerable site on the molecule (Reactive Site 2). The conjugated diene on the Adda side chain is believed to be responsible for the toxicity of mirocystins.[54] Therefore if a byproduct contains Adda functional group, it would be biologically toxic.[55] It is possible that the product may still be toxic if the conjugated diene is intact. The product with m/z 748 that was observed in both AOPs likely undergoes the loss of both triamine and Adda group (Figure 20). From there, it loses additional 16 u to form a product with m/z of 732. Neutral loss of 16 u is associated with a loss of a methyl group. There are several functional methyl groups on the molecular structure of MCs. However, the isobutyl group of MC-LR (Reactive Site 3 in Figure 19) is likely to be more accessible to an attack by a hydroxyl radical. The proposed product with m/z 732 is shown in Figure 20. The product with m/z 790 also undergoes transformation at the Adda group and the loss of a triamine. However, more of the Adda group remains on this product, as indicated by two potential bond breakage locations in Figure 19. However, the conjugated diene is likely preserved in this larger product, and it is possible that this product is still toxic. Product with m/z 674 was observed for MC-YR but not MC-LR (Figure 20). The product shows a higher degree of transformation including ring opening. Structurally, this product is likely to form with the other two MCs as well, as variable portion of the molecule (Figure 21) is lost. This is also true for the other lower molecular weight products, such as m/z 732. The reason the product with m/z 674 was observed with MC-YR but not MC-LR is because of the greater degree of parent molecule decrease was observed for MC-YR in the AOP processes, and therefore it can be expected that the products will show a higher degree of transformation, including the opening of the heptapeptide ring. Overall, parts of MCs vulnerable to hydroxyl radical attack are Adda group (with or without the loss of the conjugated diene and the toxicity associated with it), and the two variable amino acids (L, Y, and R). Further level of treatment leads to ring opening and eventual further breakdown of the molecular structure. While the product with m/z 790, or other higher molecular weight products that were not detected, may still be toxic, the overall vulnerability of the Adda group suggests that AOP will likely result in formation of non-toxic products of MCs.

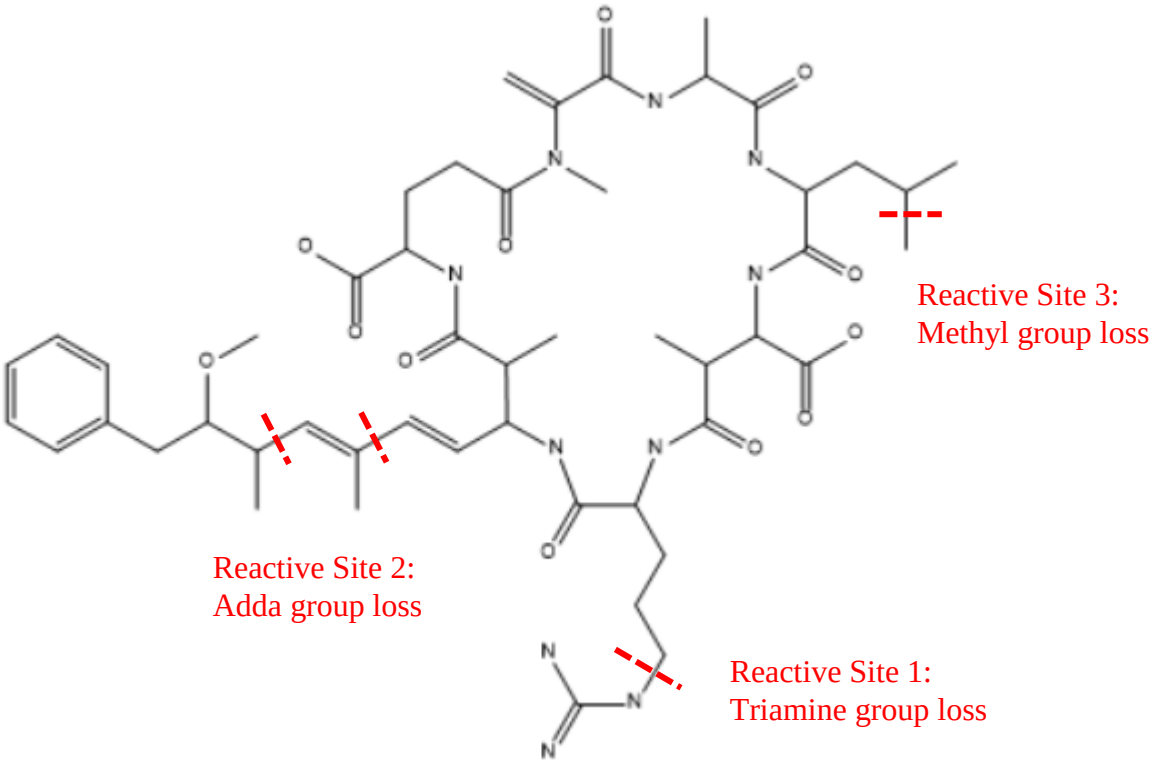

Figure 19. MC-LR structure and sites vulnerable to reaction (dashed lines indicate the sites on the molecule where bonds may break to form the transformation products.

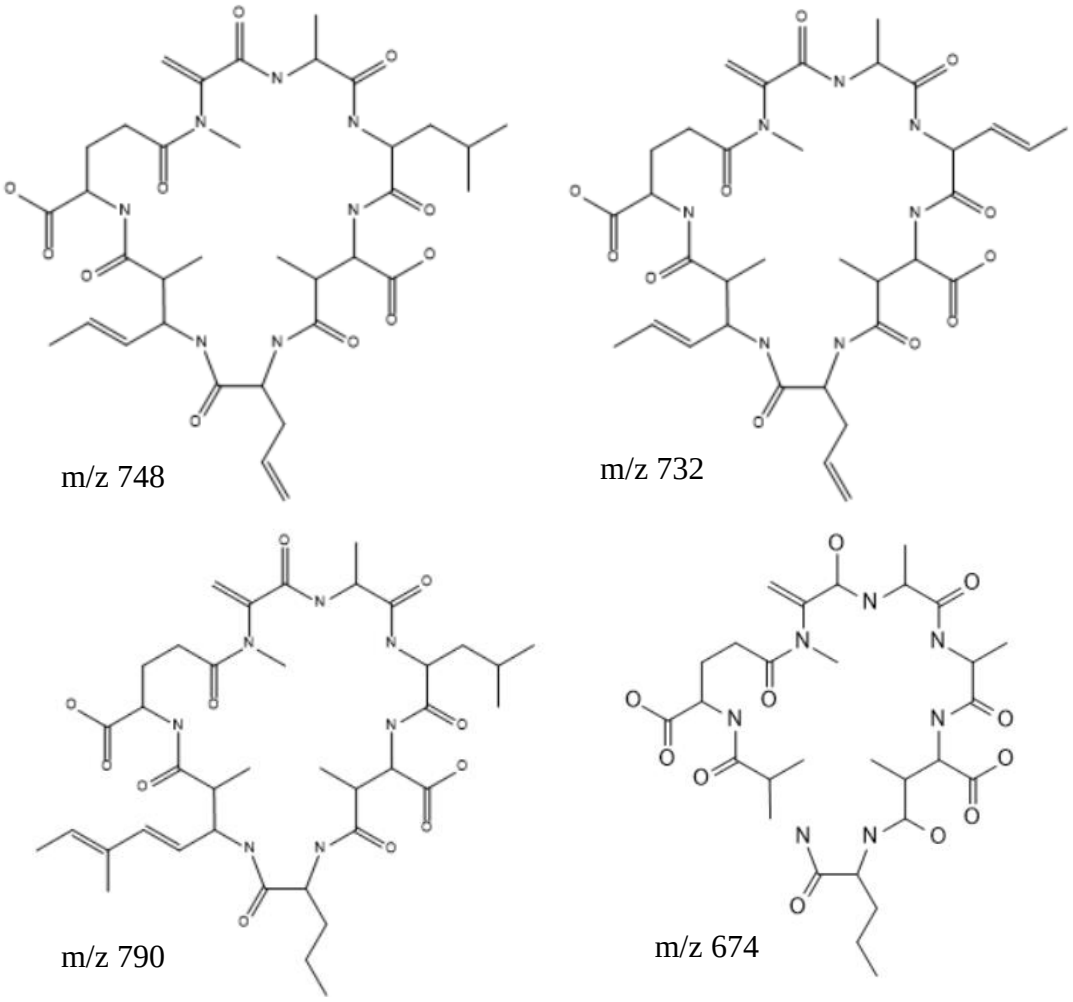

Figure 20. Proposed products of MC-LR (m/z 748, 732 and 790) and MC-YR (m/z 732, 790 and 674)

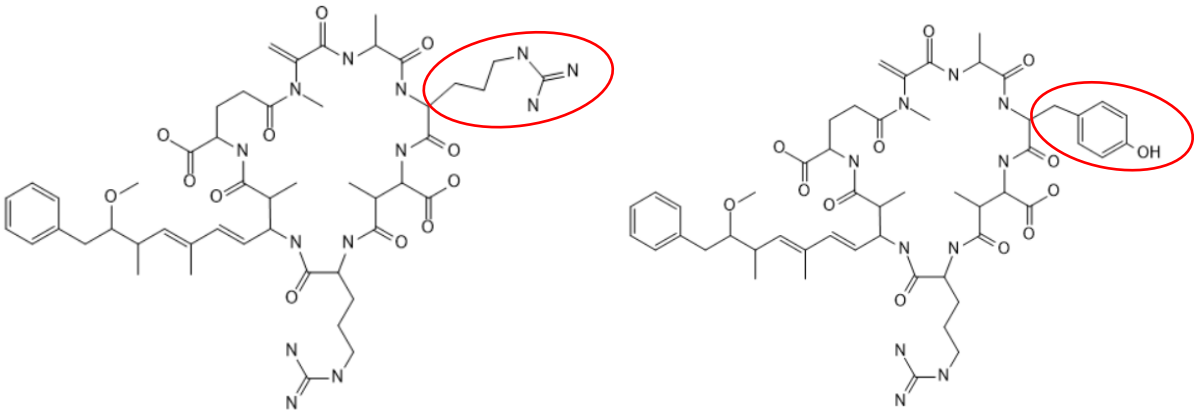

Figure 21. Structure of MC-RR (left) and MC-YR (right). Circled portion of the molecule differs between the three MCs in this study.

The effect of UV/H_2O_2 and UV/Cl_2 AOPs on formation of DBPs: The same water matrices and AOPs experiments were conducted with no added MCs to collect samples for DBP analysis. Four regulated THMs, nine regulated HAAs, and NDMA were analyzed.

For THMs and HAAs analysis, Liu and the research team optimized the critical factors in the derivatization step including the volume and concentration of acidic methanol, the amount and concentration of Na_2SO_4 solution, the volume of saturated $NaHCO_3$ solution, and derivatization time and temperature.[45] The following results on THMs and HAAs formation are based on their findings on the optimum extraction method. The data are average values of triplicate samples.

For post-AOP tests such as toxicity assays or mass spectrometry, enzymatic options are recommended quench H_2O_2.[39] Therefore, bovine catalase was used to quench H_2O_2 in MCs AOPs experiences that were followed by LC/MS-MS and PP2A analysis. For the samples that include chlorinated DBP analysis chlorine is the recommended option to quench H_2O_2.[39] UV/H_2O_2 samples needed higher chlorine dose compared to UV/Cl_2 samples to achieve same residual chlorine as residual H_2O_2 readily reacts with Cl_2. The reaction between chlorine and H_2O_2 is much faster than the reaction between chlorine and DOM.[39] Consequently, a slight increase to no increase in DBP formation was expected in UV/H_2O_2 samples because of the increased initial chlorine dose required to quench H_2O_2.[39]

Trihalomethanes: Figures 22-29 show the effect of matrices and UV dose for different AOP processes on THMs formation and comparison of AOPs at given UV dose for different matrices for each THM.
In most cases, the water matrix, UV dose, oxidant dose, and different processes (UV/Cl_2 vs. UV/H_2O_2) did not show a significant effect on the four THMs that were studied. Chloroform increased with algal DOM presence in hydrogen peroxide processes (Figure 22). According to the t-test, which compared the results of background water matrix to that with added AOM, the p-value at 95% confidence level was 0.028 indicating that the results were significantly different. Also, chloroform was suppressed by nitrate and the p-value was 0.066 which was not statically significant (but close to p-value of 0.05 below which the results are statistically significant). In UV/H_2O_2 processes, comparing two series of data at different UV doses, the increase in the concentration of hydrogen peroxide decreases the chloroform formation. However, the changes were not statistically significant with the p-values equal to 0.226, 0.134, and 0.135 in background, matrix with nitrate, and matrix with AOM, accordingly. The contribution of AOM in chloroform formation is more explicit in Figure 23.

Algal DOM also increased the formation of bromodichloromethane in UV/H_2O_2 process significantly with the p-value of 0.019 under H_2O_2= 5 mg/L (Figure 24).

The maximum contaminant level (MCL) of total THMs (TTHMs) in the treated water is 80 µg/L. In this study, the maximum TTHM concentration was 46.26 µg/L belonging to the background matrix that was treated using Cl_2 = 4 mg/L and UV = 2000 mJ/cm^2, which is much less than the MCL (Figures 30 and 31).

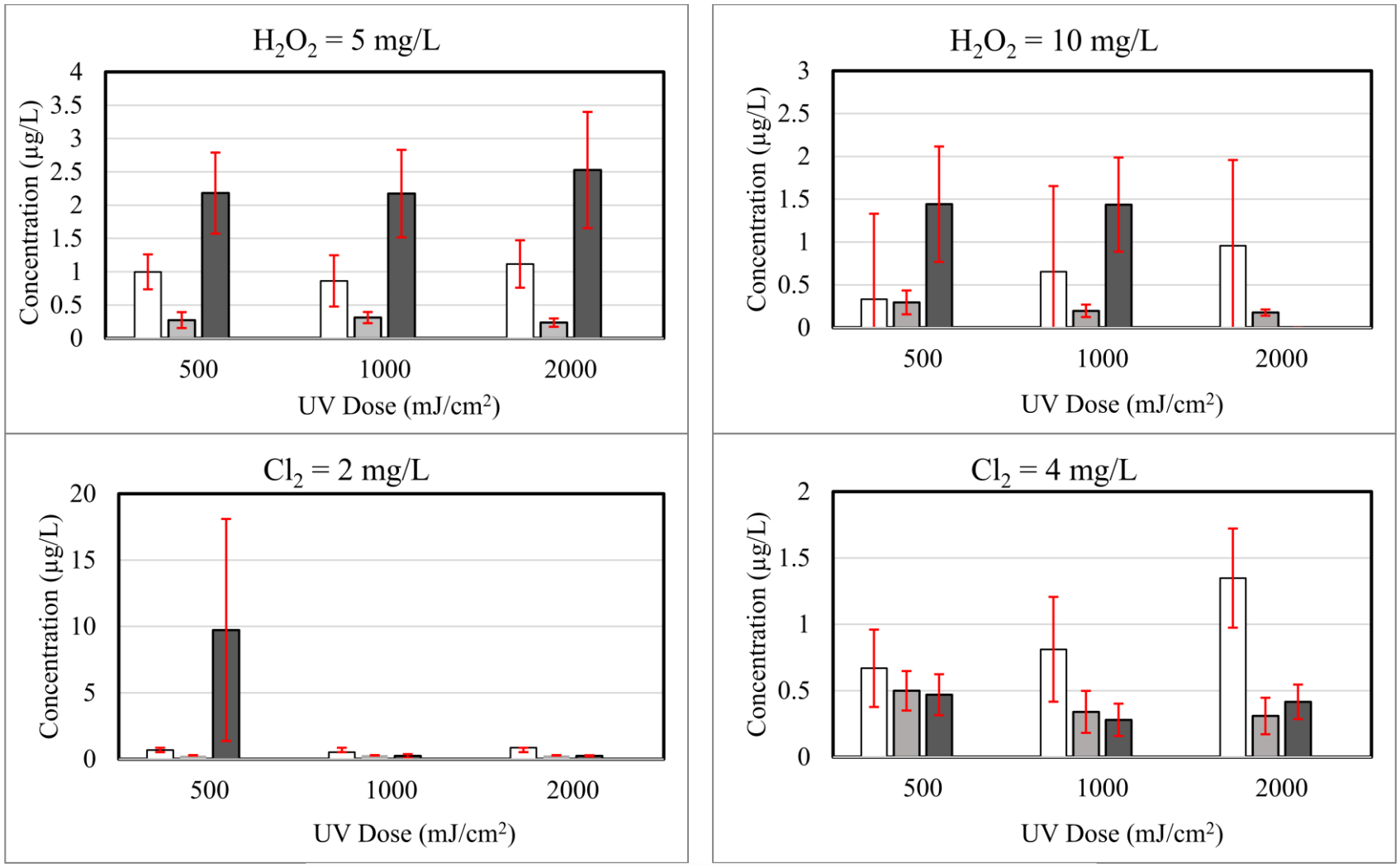

Figure 22. Effect of matrix and UV dose for different processes on chloroform.
Figure shows the average of three separate experiments with the error bars showing standard deviation.

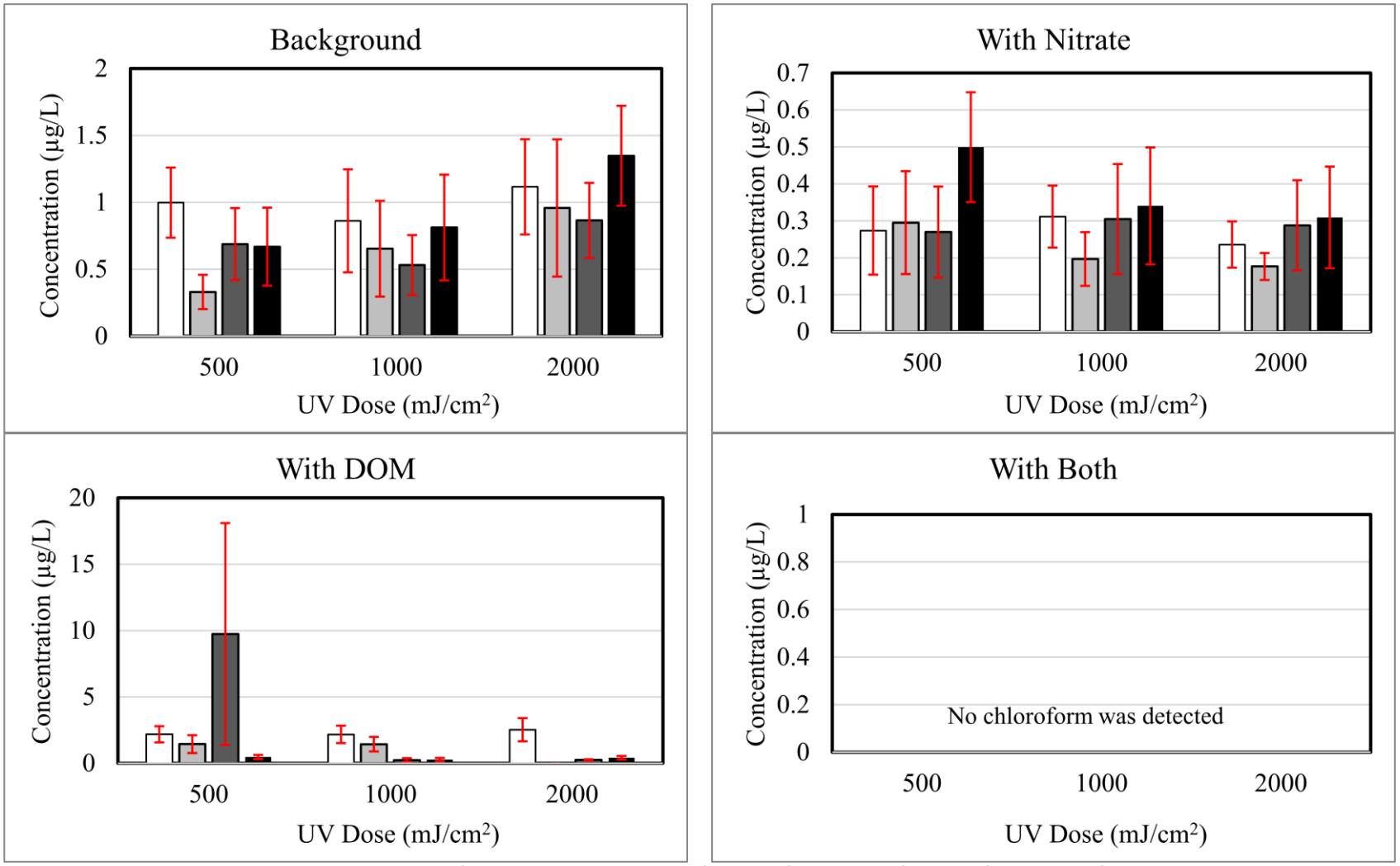

Figure 23: Effect of processes at a given UV dose and matrix on chloroform formation.
Figure shows the average of three separate experiments with the error bars showing standard deviation.

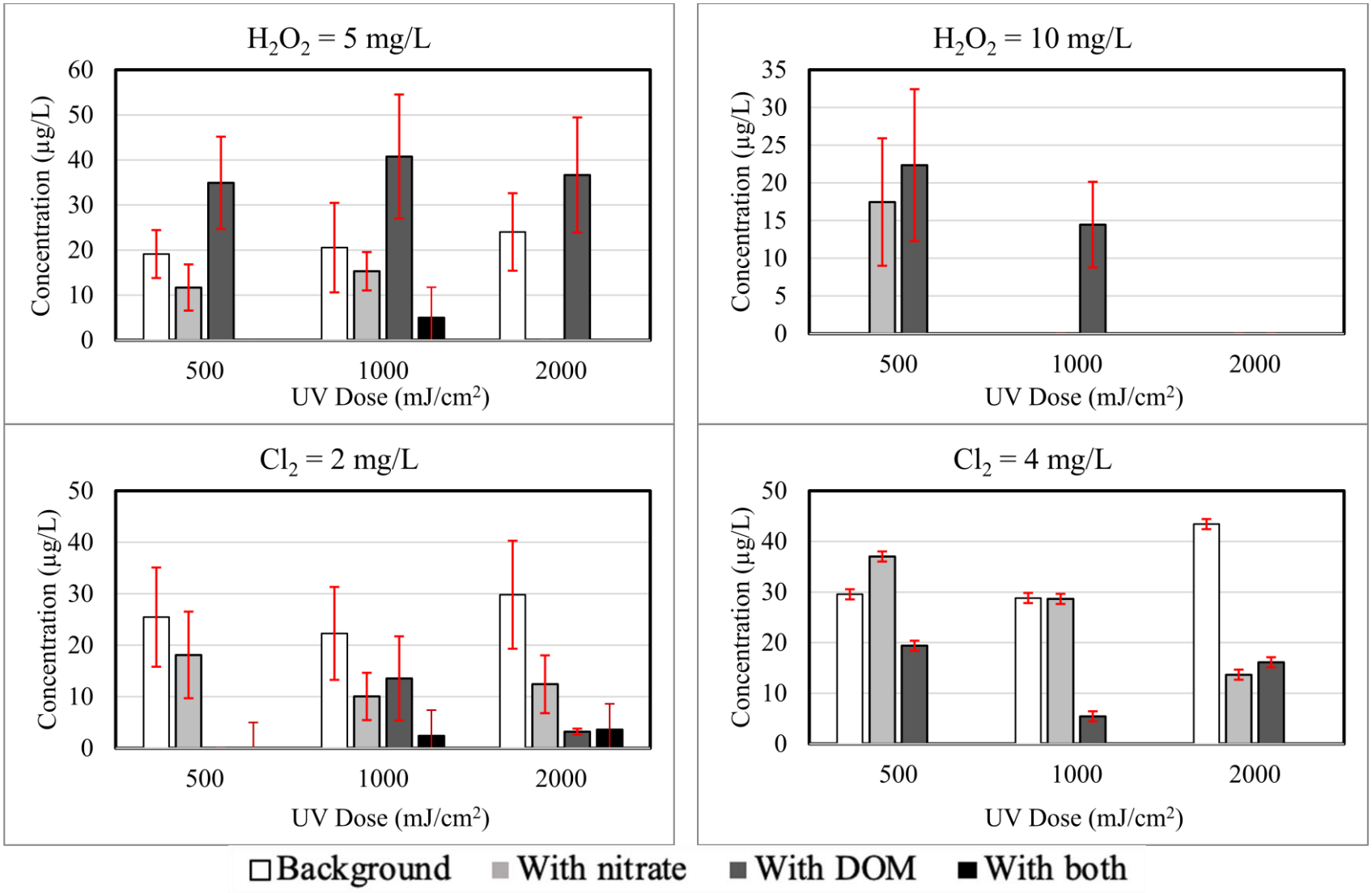

Figure 24. Effect of matrix and UV dose for different processes on bromodichloromethane formation. Figure shows the average of three separate experiments with the error bars showing standard deviation.

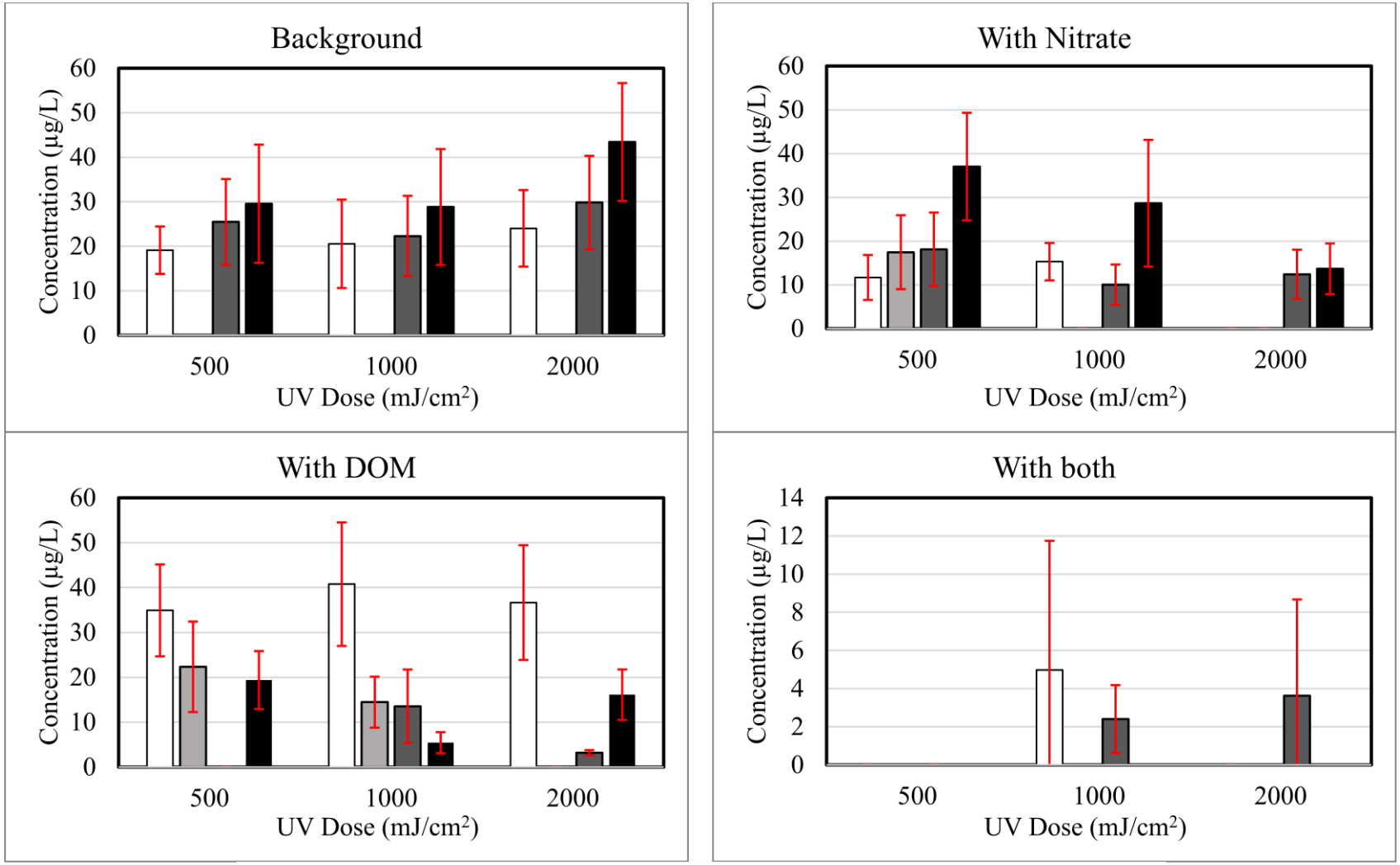

Figure 25. Effect of processes at a given UV dose and matrix on bromodichloromethane formation. Figure shows the average of three separate experiments with the error bars showing standard deviation.

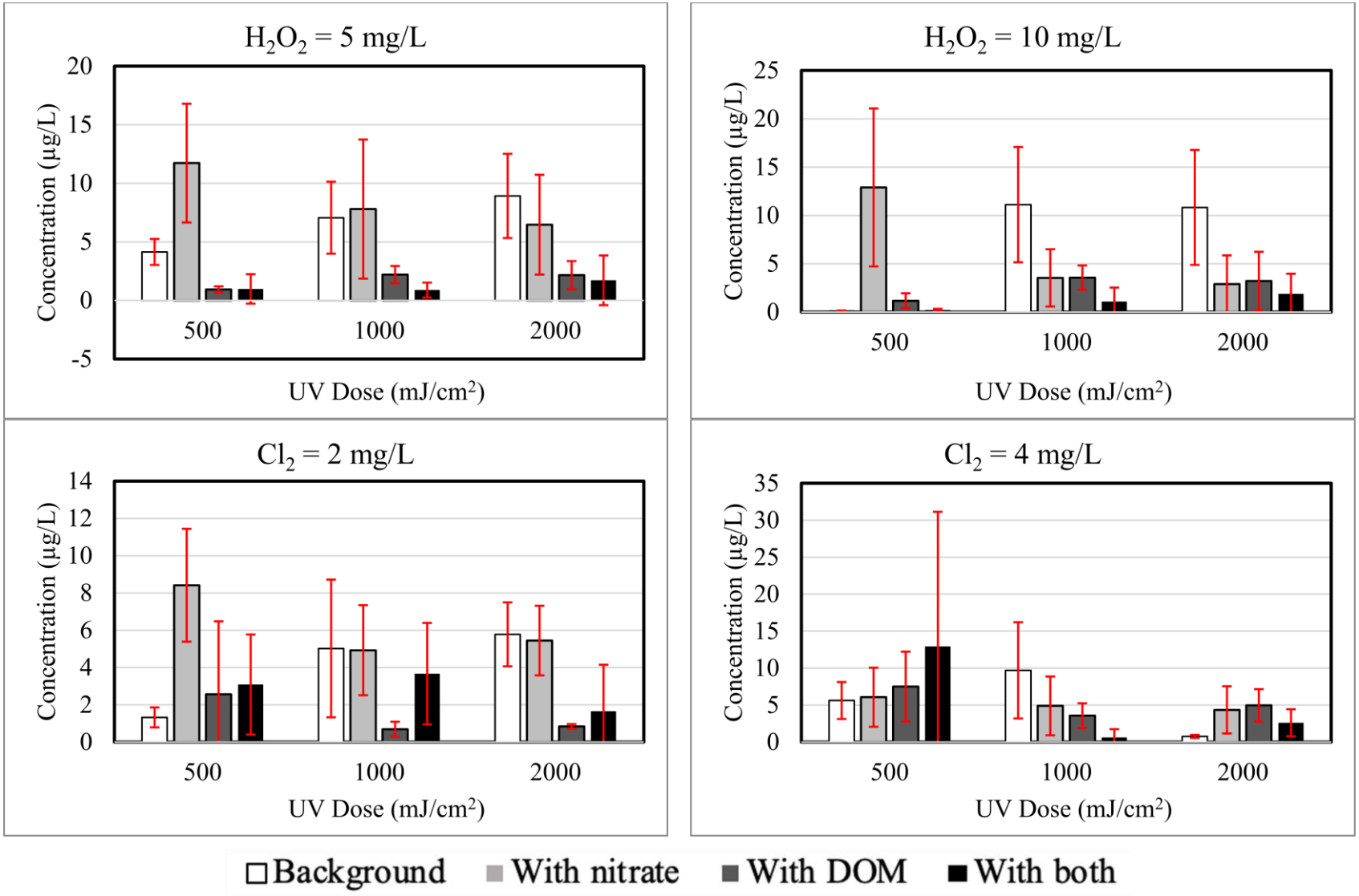

Figure 26. Effect of matrix and UV dose for different processes on dibromochloromethane formation. Figure shows the average of three separate experiments with the error bars showing standard deviation.

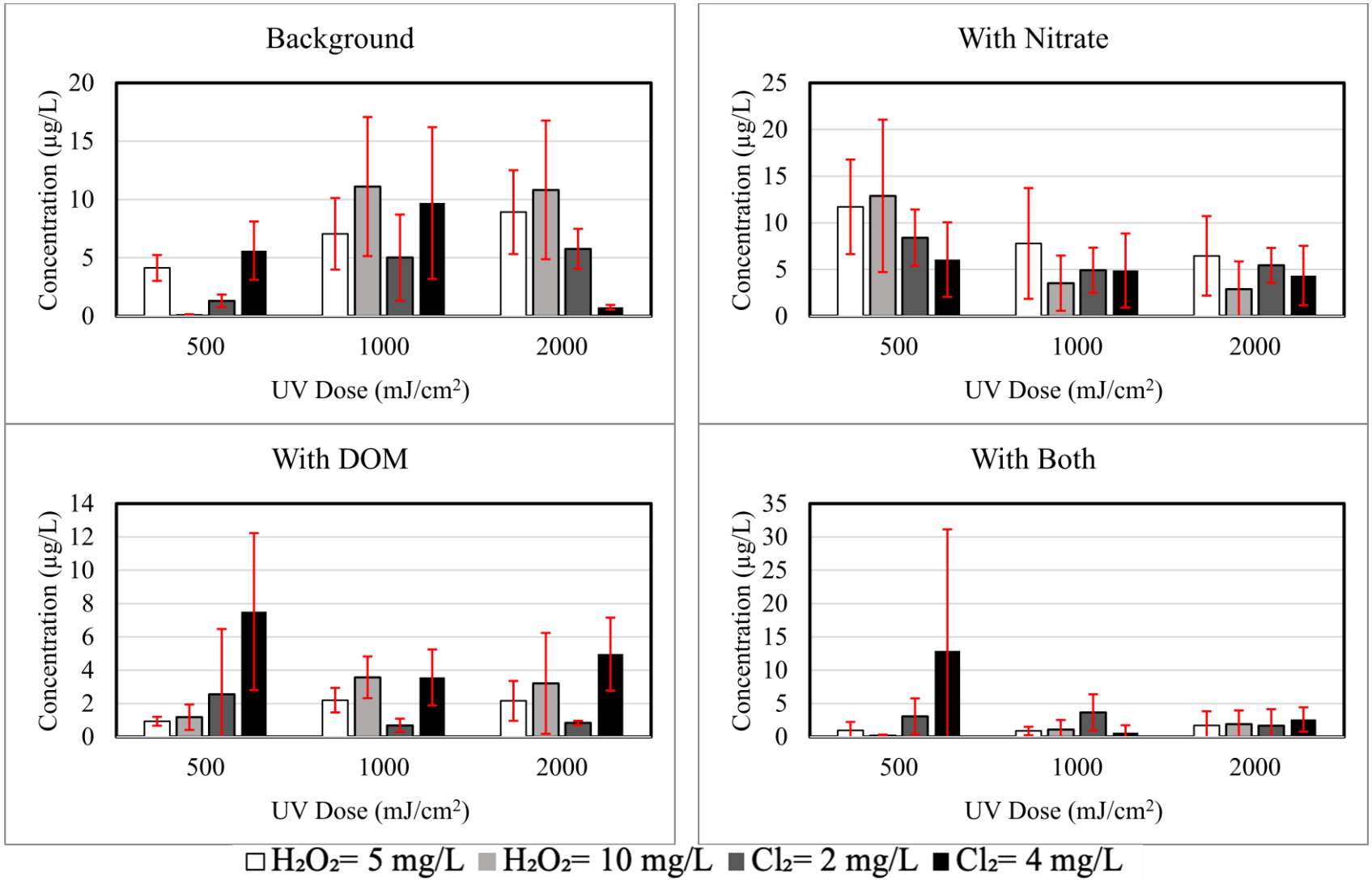

Figure 27: Effect of processes at a given UV dose and matrix on dibromochloromethane formation. Figure shows the average of three separate experiments with the error bars showing standard deviation.

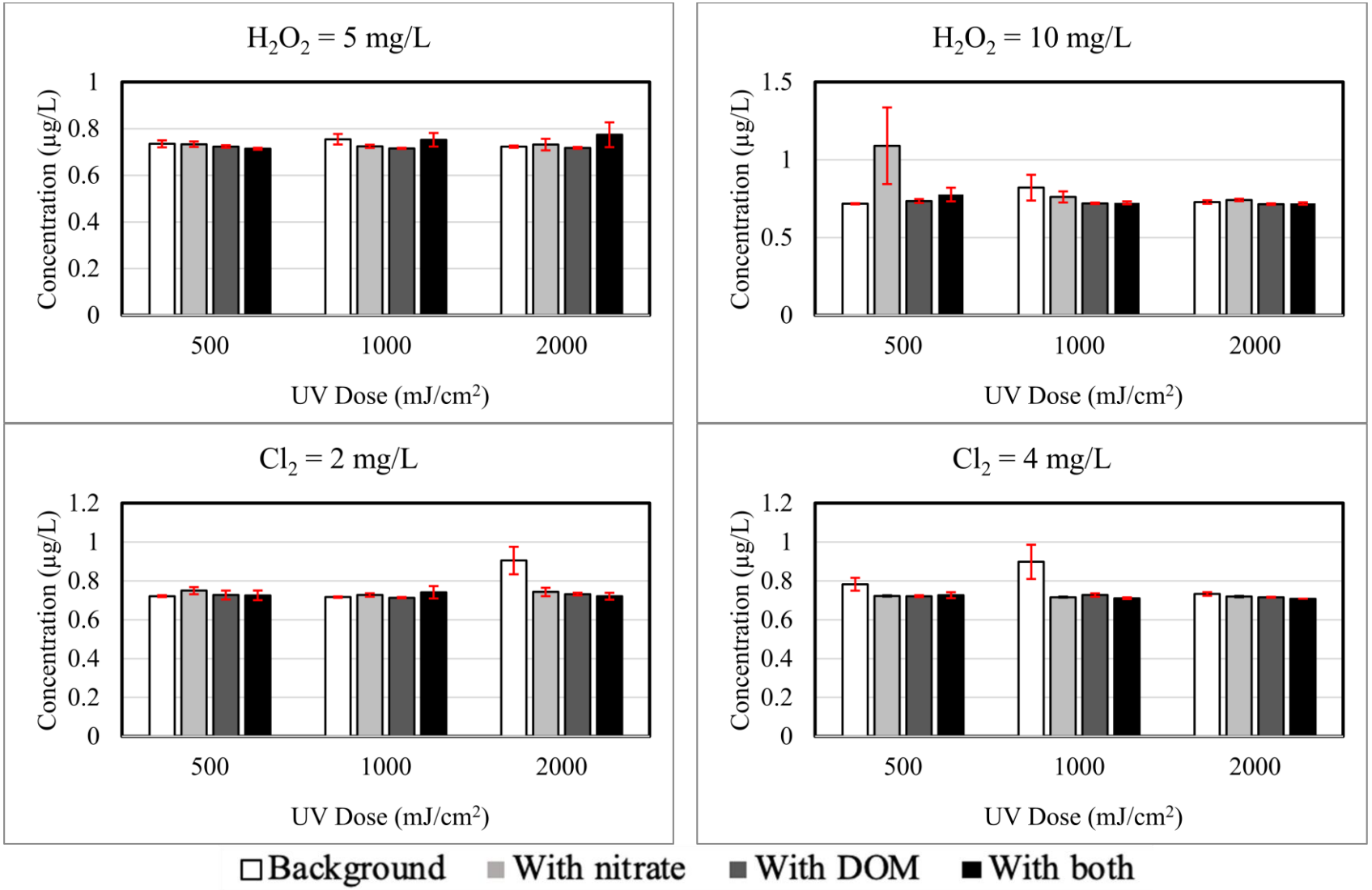

Figure 28. Effect of matrix and UV dose for different processes on bromoform formation.
Figure shows the average of three separate experiments with the error bars showing standard deviation.

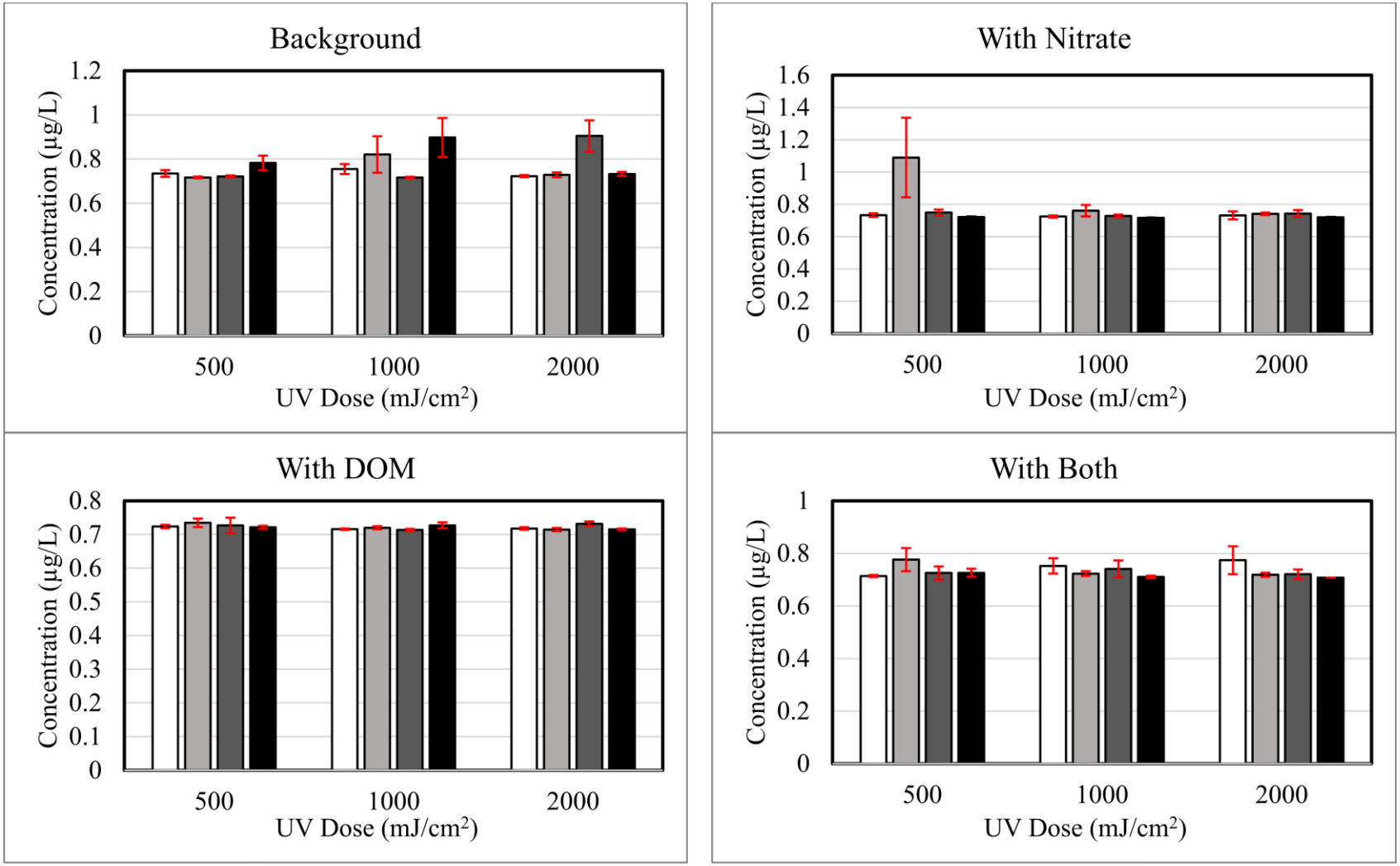

Figure 29: Effect of processes at a given UV dose and matrix on bromoform formation.
Figure shows the average of three separate experiments with the error bars showing standard deviation.

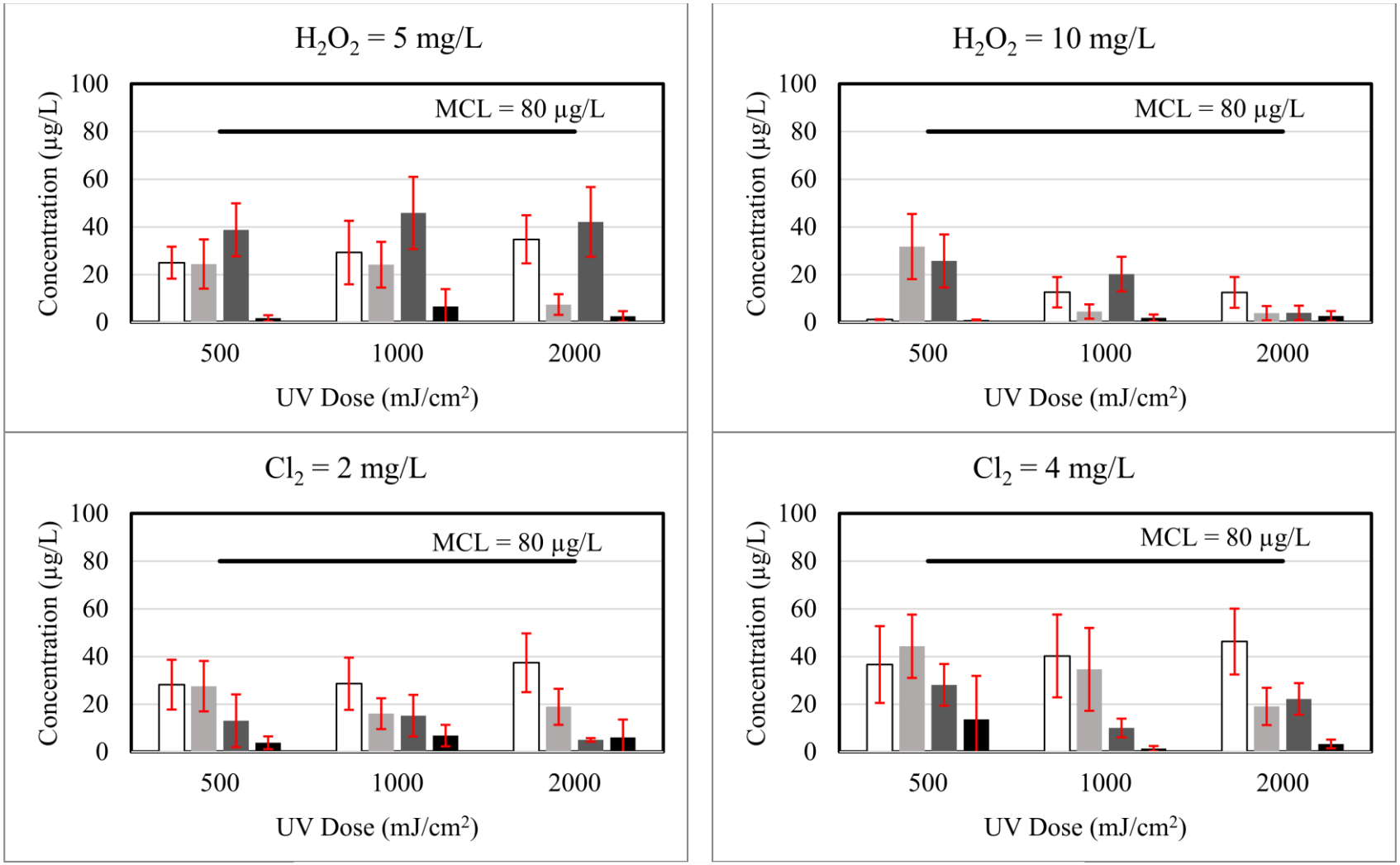

Figure 30. Effect of matrix and UV dose for different processes on TTHMs formation.
Figure shows the average of three separate experiments with the error bars showing standard deviation.

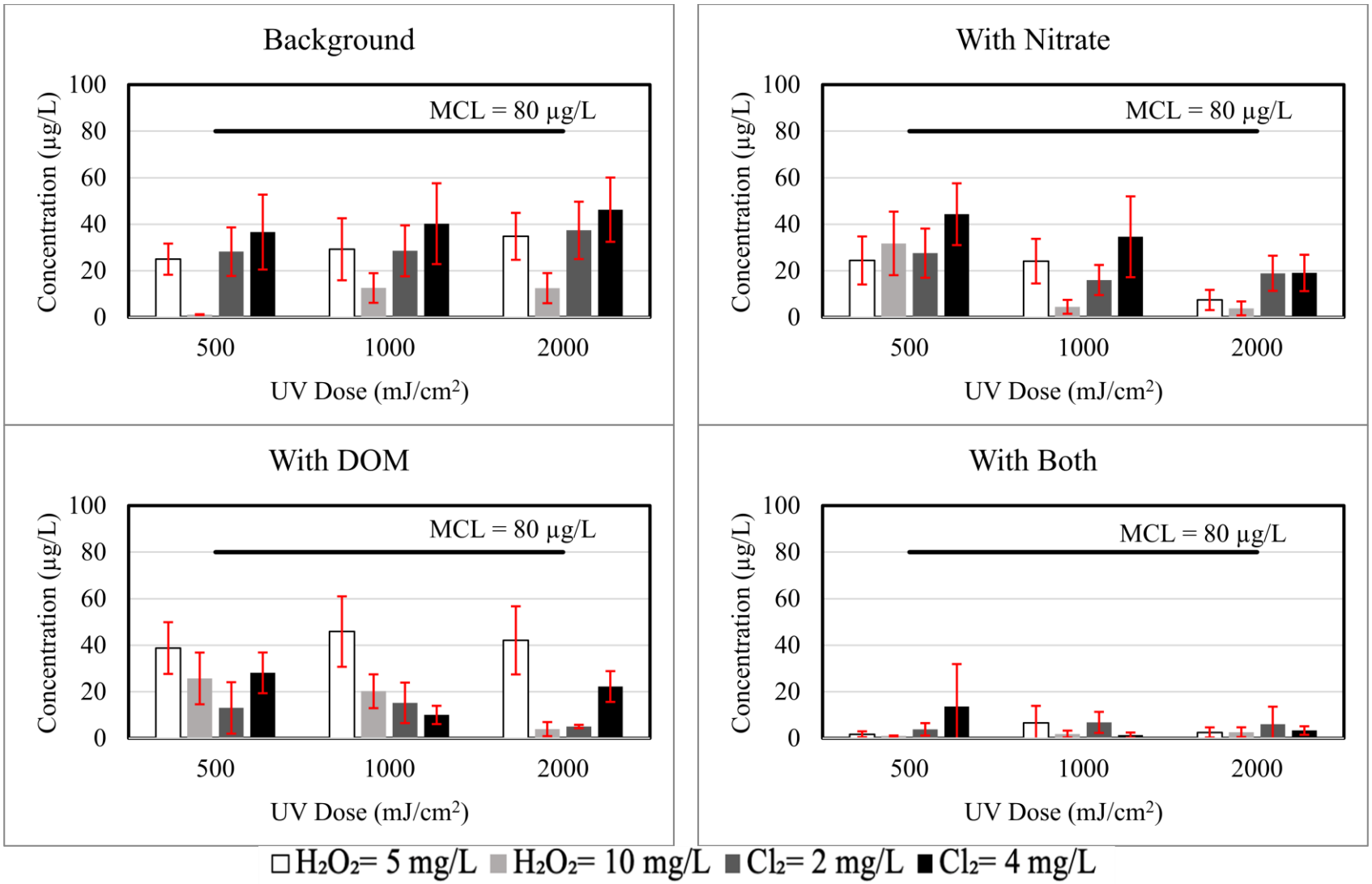

Figure 31: Effect of processes at a given UV dose and matrix on TTHMs formation.
Figure shows the average of three separate experiments with the error bars showing standard deviation.

Haloacetic acids: Nine HAAs were studied in this project, among which only three HAAs were detected in the treated samples: tribromoacetic acid (Figures 31-32), monochloroacetic acid (Figures 33-34), and chlorodibromoacetic acid (Figures 35-36). The sample matrix impacted HAA formation. Specifically, tribromoacetic acid formation was higher in samples containing nitrate (Figure 32). However, the difference was not statistically significant, and the p-value was 0.130 and 0.120 for UV/H_2O_2 and UV/Cl_2, respectively, for matrices with or without additional nitrate. Monochloroacetic acid formed during UV/H_2O_2 processes was significantly suppressed by the addition of nitrate and algal DOM to the background matrix (Figure 35). The p-values were 0.039 and 0.035 for matrix with nitrate and matrix with DOM, respectively, as compared to the background matrix.

No correlation was observed between the type of process or the level of treatment and HAA formation.

The MCL of total HAAs (THAAs) is 60 µg/L in drinking water. In this study, the maximum total HAAs was 127.8 µg/L belonging to matrix containing 20 mg/L NO_3 treated by H_2O_2 5 mg/L under UV = 1000 mJ/cm^2. However, in most of the samples total HAAs concentration was less than MCL (Figures 37-38) and only seven samples exceed the MCL. The background water matrix had a relatively high bromide concentration (0.105 mg/L) due to the presence of coal burning power plants upstream in the watershed of the Catawba River. High bromide leads to higher formation of brominated DBPs that contribute to higher TTHMs and THAAs because of the larger molecular weight than chlorinated DBPs. Overall, bromide incorporation in this study was 38% on average and ranged from 8 to 100%. The samples with higher bromide incorporation were the ones exceeding the MCL. However, no obvious correlation between bromide incorporation and the matrix or treatment processes was observed. No trends were present with increasing UV doses. The sample with the highest bromide incorporation (two samples with 100% incorporation), were both in UV/H_2O_2 AOP with nitrate-spiked matrix. Addition of nitrate and AOM appeared to increase the bromide incorporation on average, but not in a statistically significant way. The average and the standard deviation for all of the background matrix samples, nitrate-spiked, AOM-spiked and nitrate+AOM samples are 29±11%, 50±29%, 36±17%, and 36±25%, respectively. Percent bromide incorporation is consistent with previous studies on this subject.[56,57]

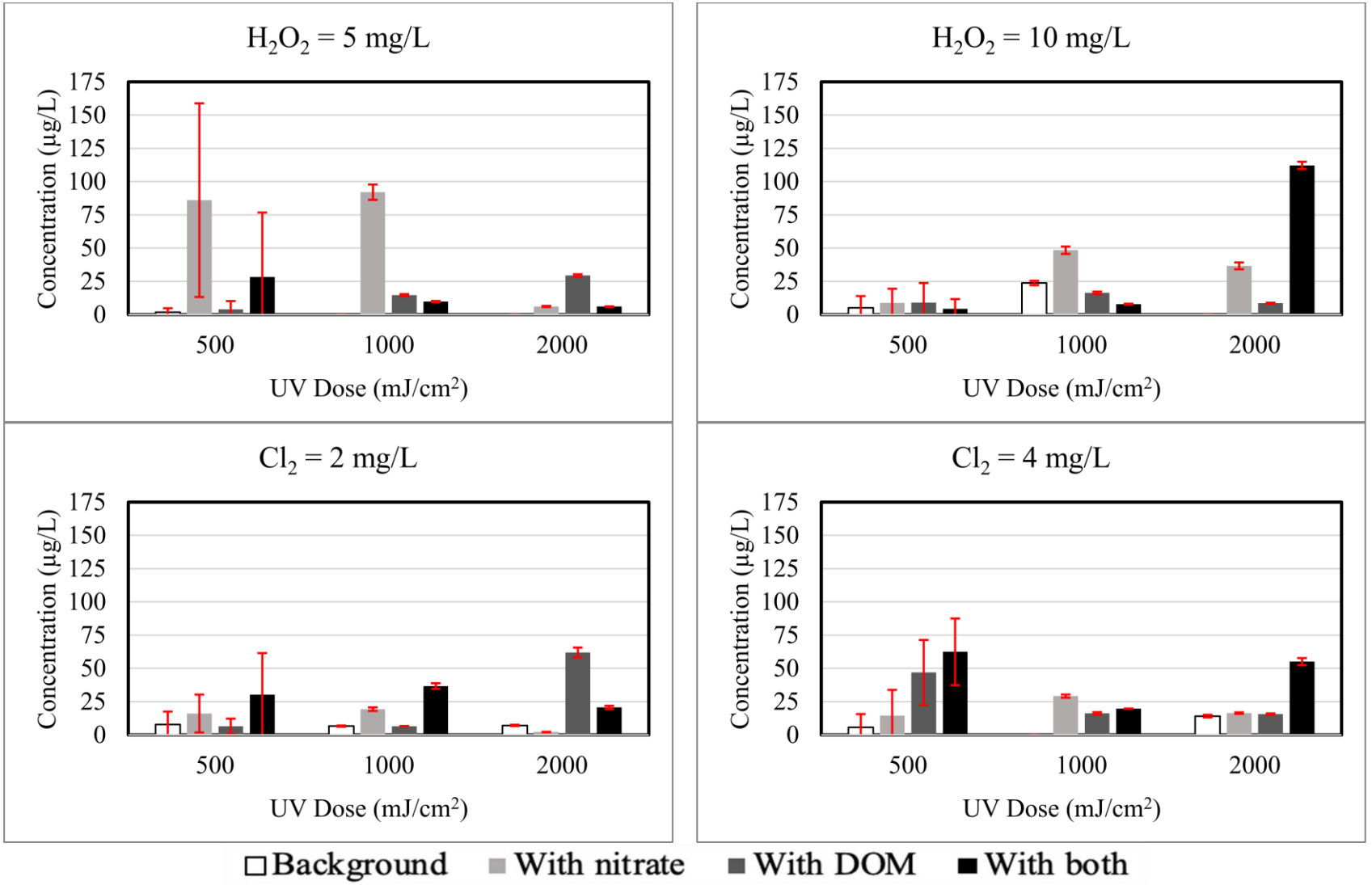

Figure 32. Effect of matrix and UV dose for different processes on tribromoacetic acid formation
Figure shows the average of three separate experiments with the error bars showing standard deviation.

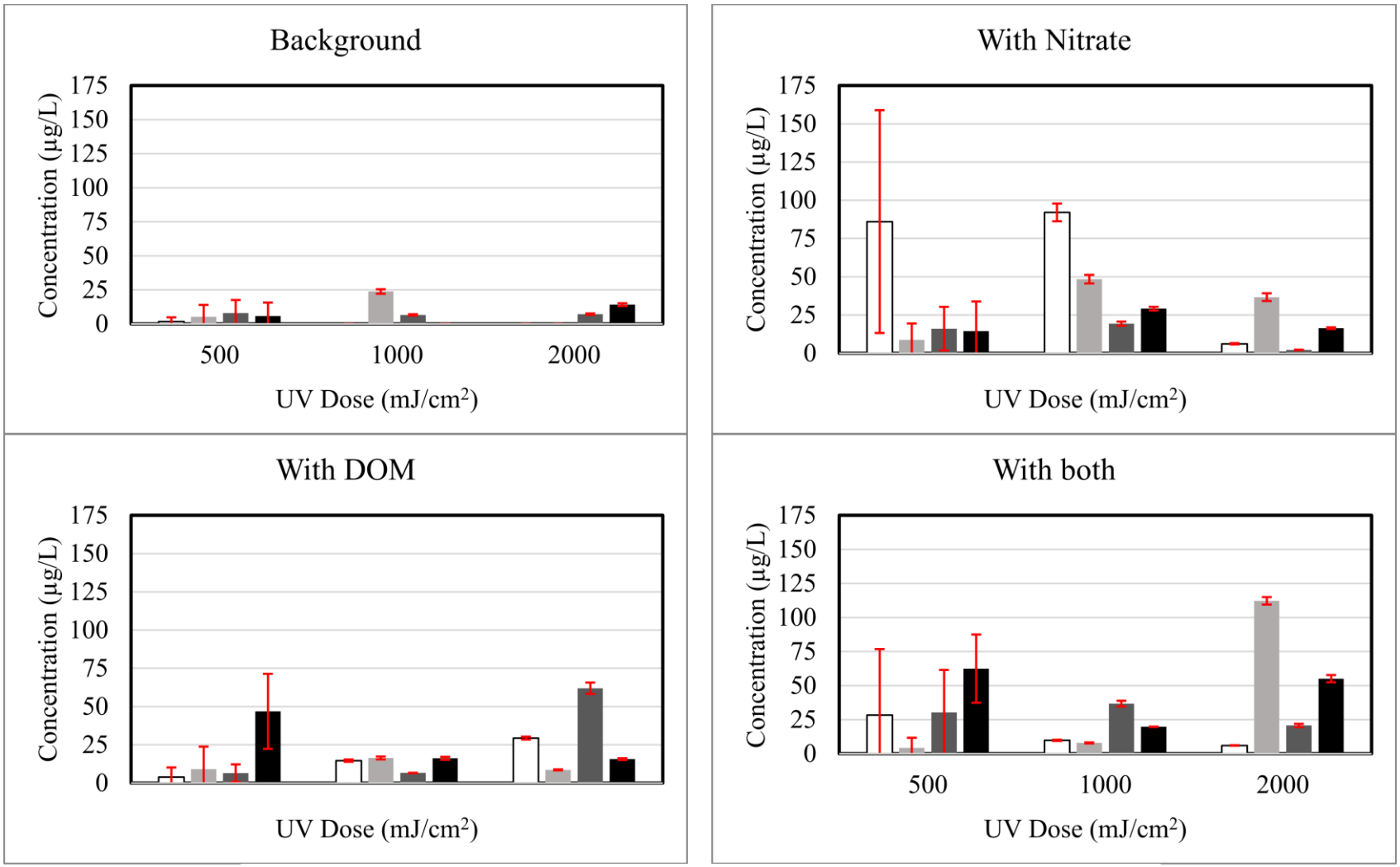

Figure 33. Effect of processes at given UV dose and matrix on tribromoacetic acid formation
Figure shows the average of three separate experiments with the error bars showing standard deviation.

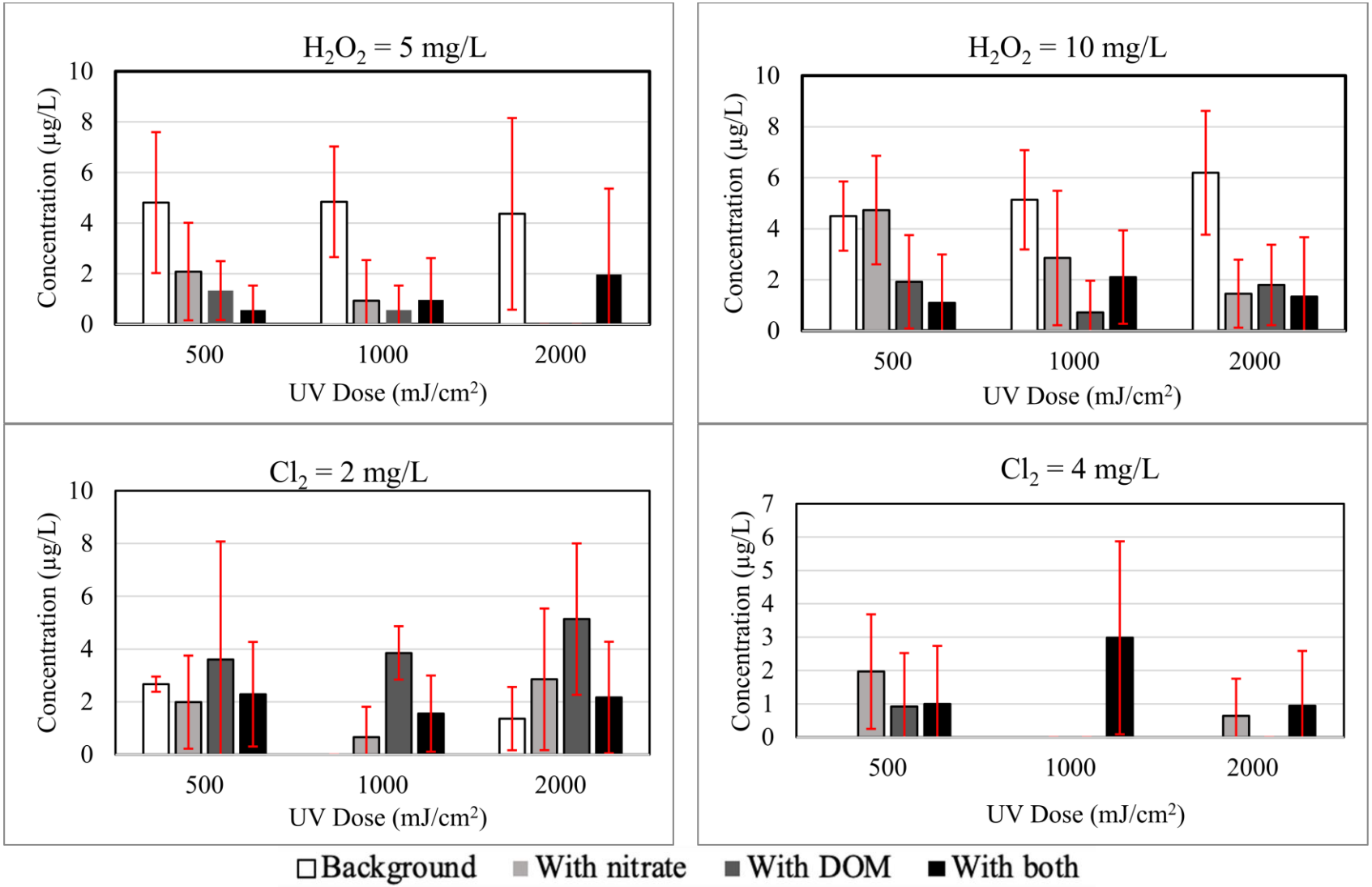

Figure 34. Effect of matrix and UV dose for different processes on monochloroacetic acid formation
Figure shows the average of three separate experiments with the error bars showing standard deviation.

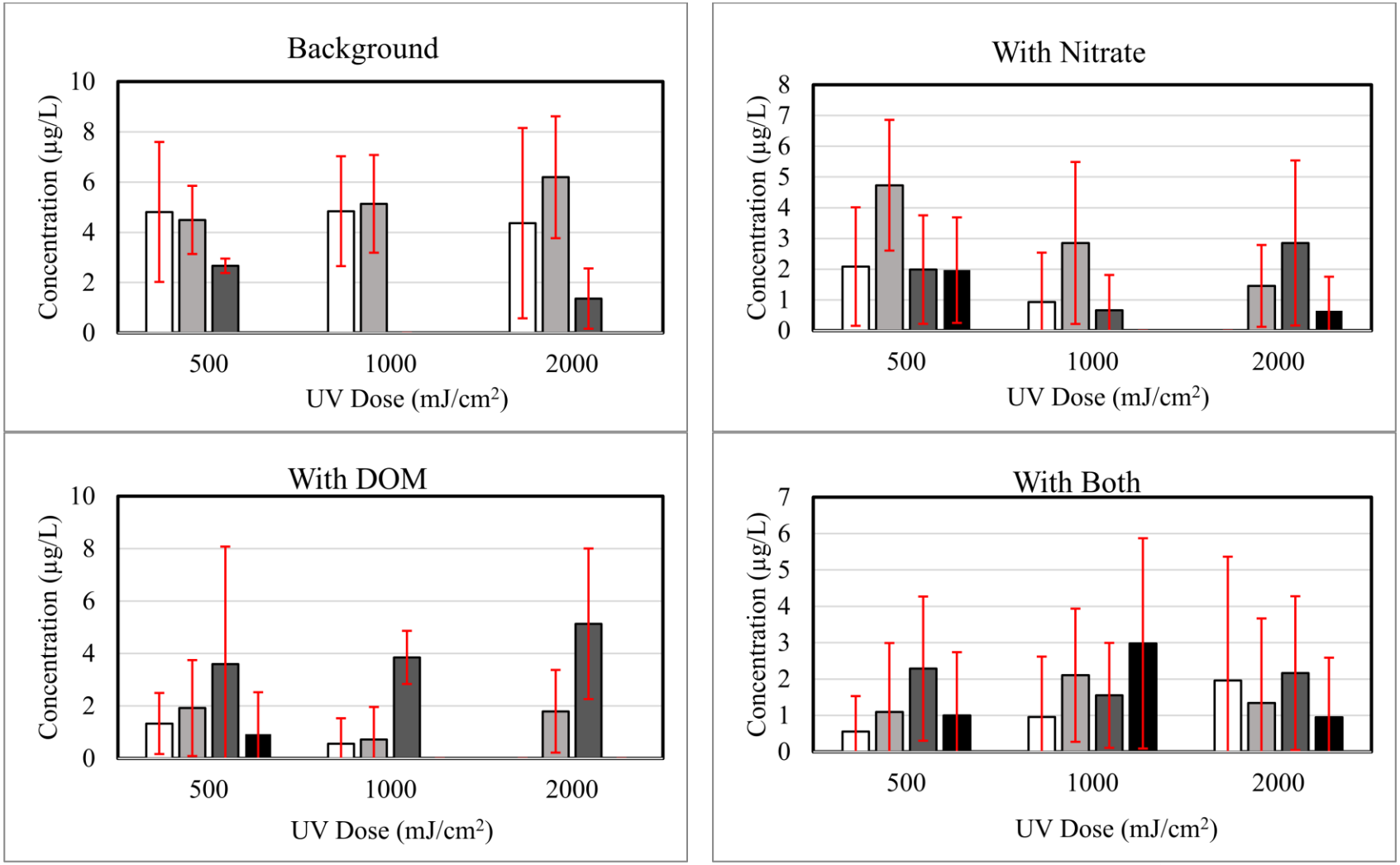

Figure 35. Effect of processes at a given UV dose and matrix on monochloroacetic acid formation
Figure shows the average of three separate experiments with the error bars showing standard deviation.

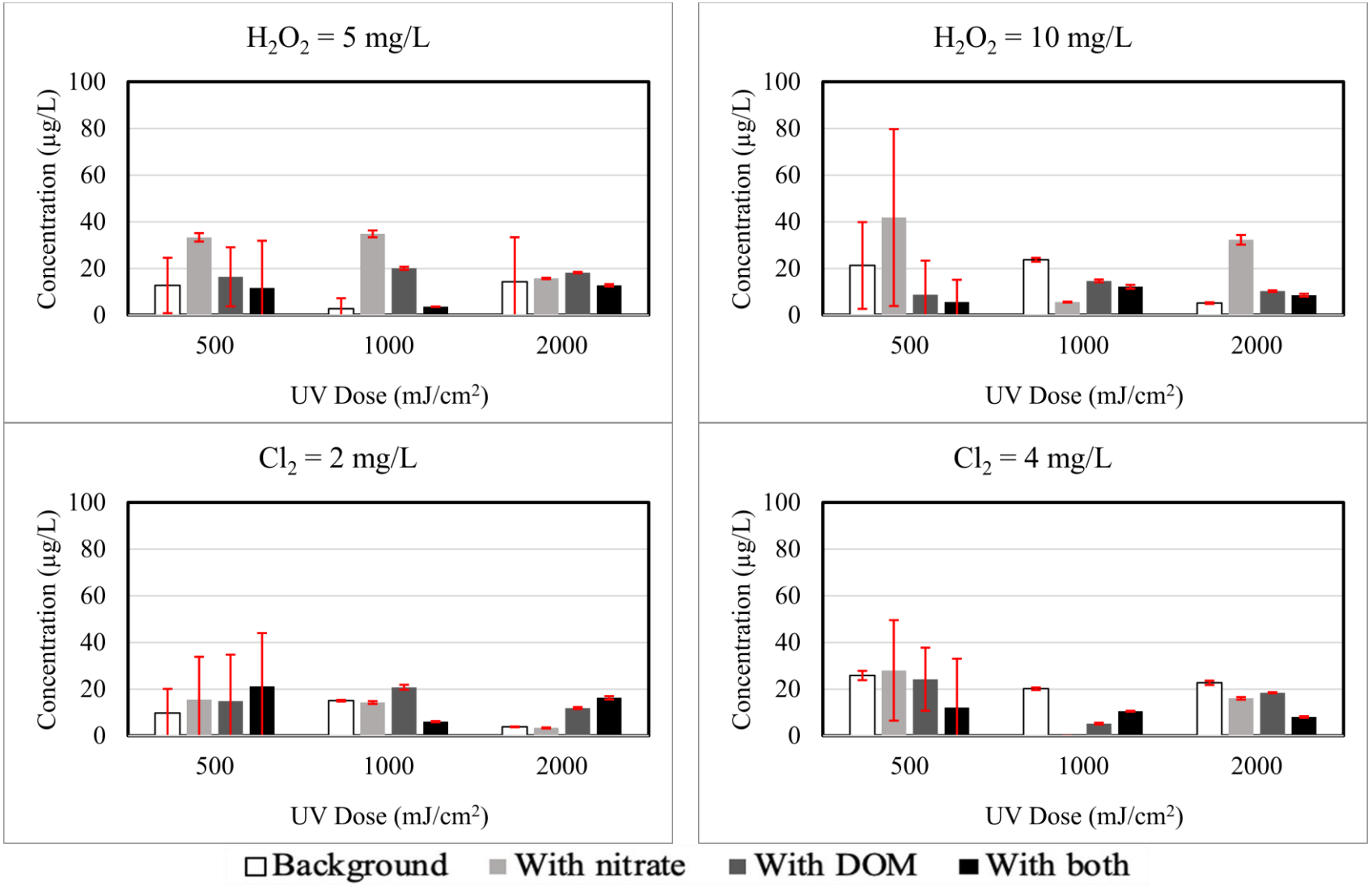

Figure 36. Effect of matrix and UV dose for different processes on chlorodibromoacetic acid formation
Figure shows the average of three separate experiments with the error bars showing standard deviation.

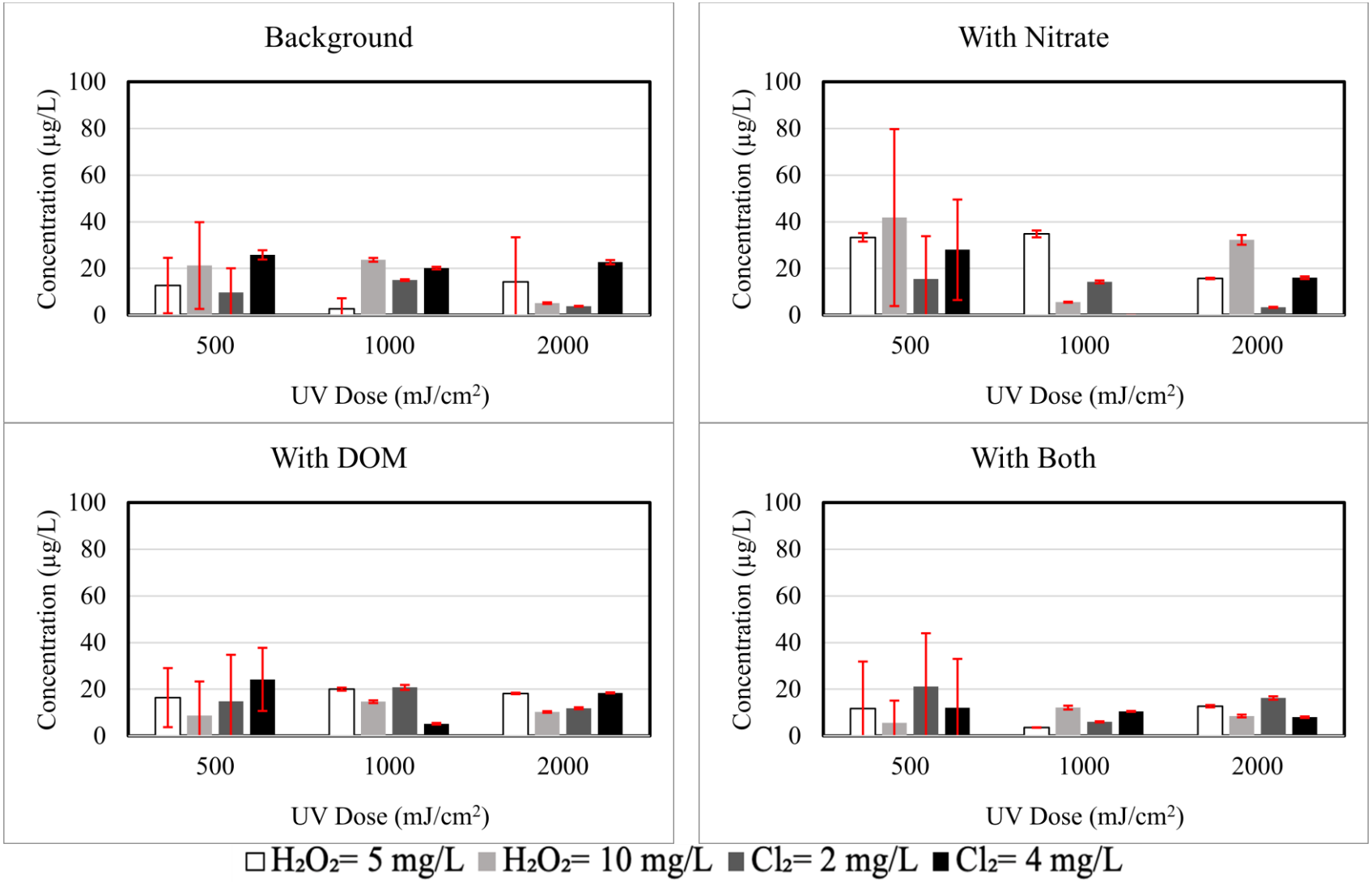

Figure 37. Effect of processes at a given UV dose and matrix on chlorodibromoacetic acid formation. Figure shows the average of three separate experiments with the error bars showing standard deviation.

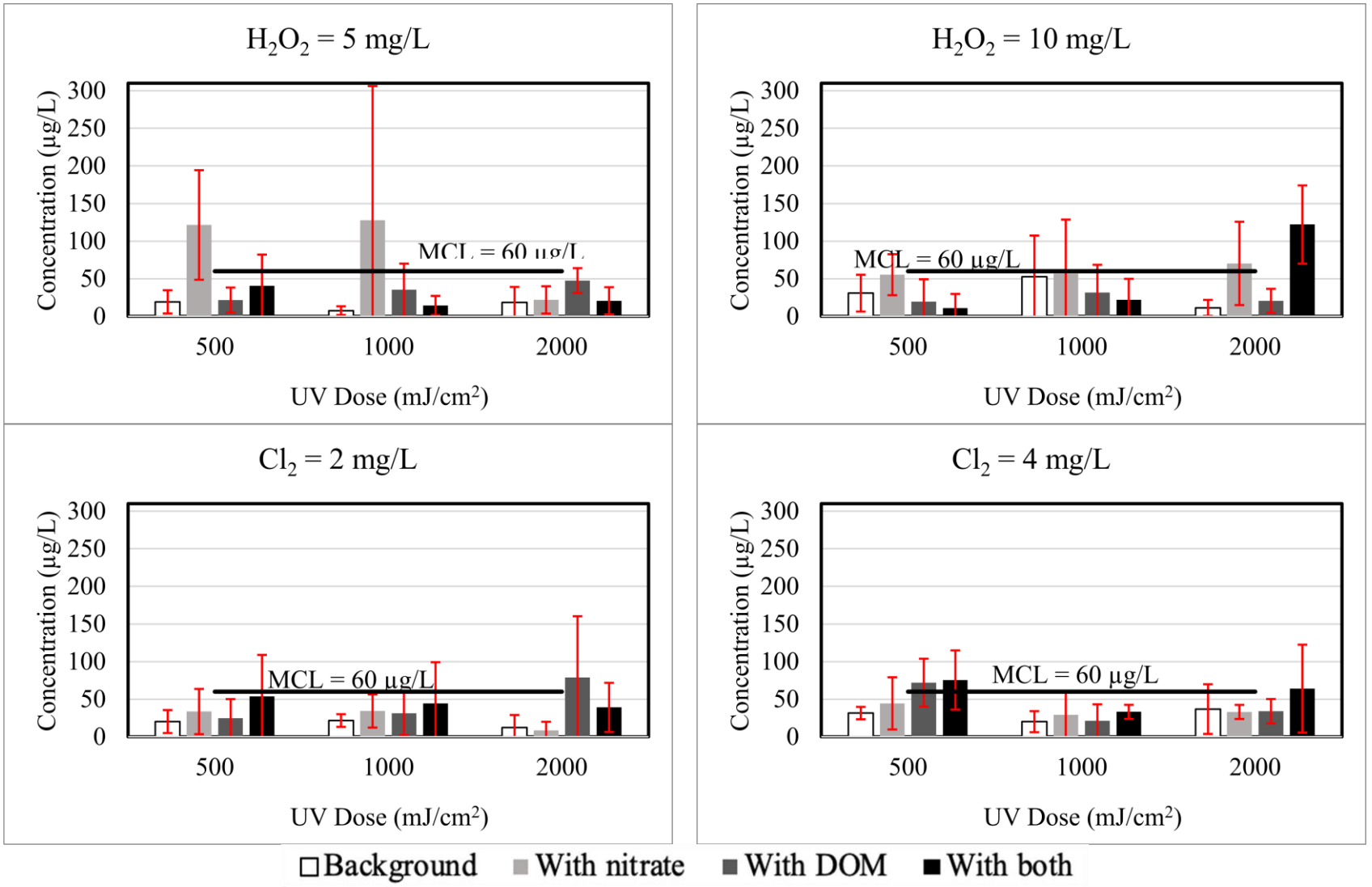

Figure 38. Effect of matrix and UV dose for different processes on THAAs formation
Figure shows the average of three separate experiments with the error bars showing standard deviation.

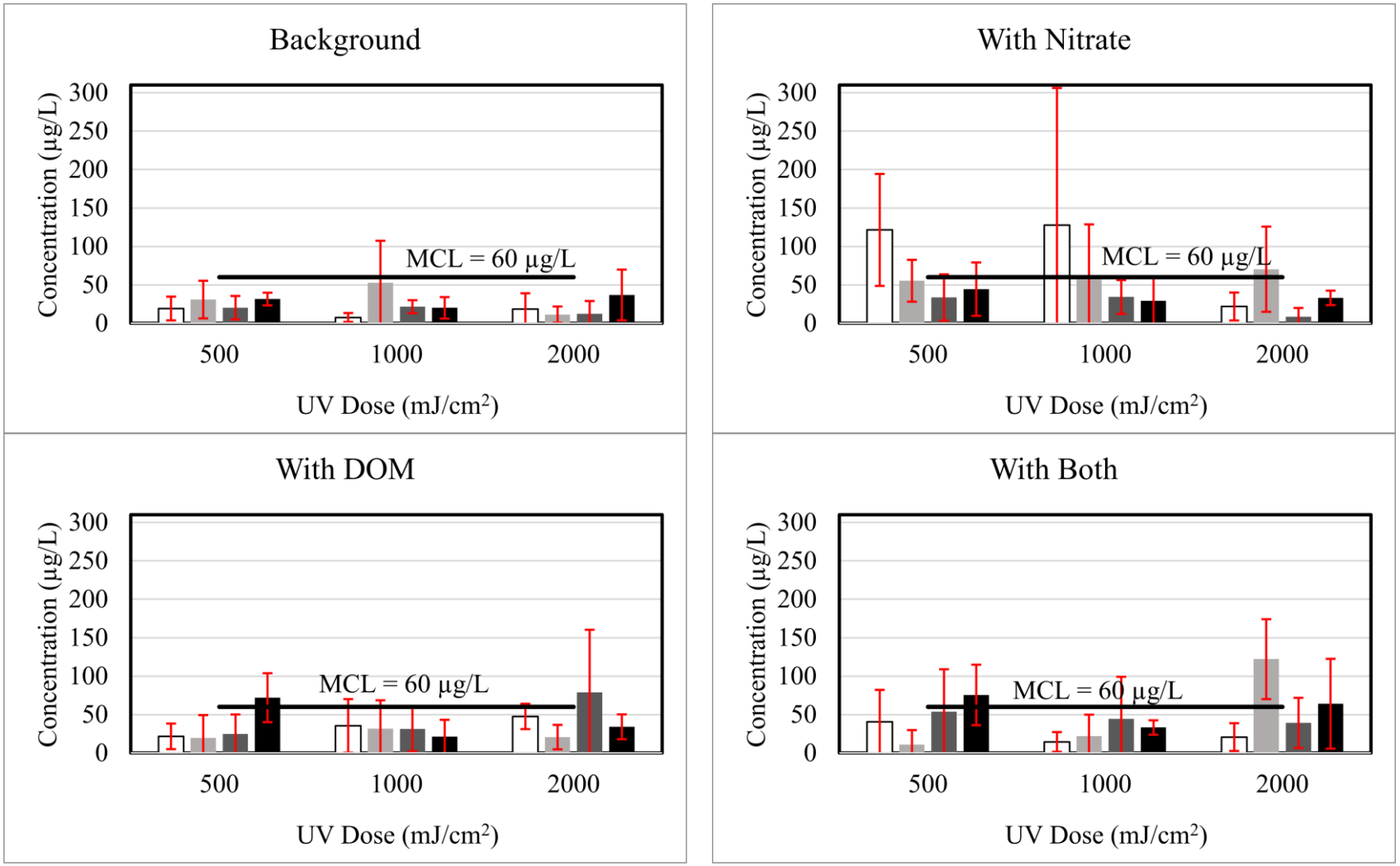

Figure 39. Effect of processes at a given UV dose and matrix on THAAs formation.
Figure shows the average of three separate experiments with the error bars showing standard deviation.

***N*-nitrosodimethylamine (NDMA):** Both nitrate and algal DOM increased NDMA formation significantly when the samples were treated by UV/H_2O_2 and the p-values were 0.050 and 0.021 for matrix with nitrate and matrix with DOM, respectively, as compared to the background matrix. Same changes were observed using UV/Cl_2 process, however, they were not statistically significant and the p-values were 0.084 and 0.123 for the matrices with additional nitrate and with additional DOM, respectively. In all cases, the NDMA was lower than the USEPA health-related advisory level of 10 ng/L.

Algal DOM is very nitrogen-rich, which explains additional formation of NDMA. C:N ratio (mass) for the algal DOM in this study was 2.5, compared to 5.6 ratio of the background matrix or, for example, 7.9 reported in another study that reported composition of surface water NOM.[58] Nitrate forms reactive nitrogen species, and it is possible that nitrite radicals can add to the structure of background organic matter providing nitroso groups that become part of nitrosamines when it reacts with organic amines in the water. It must be noted, however, that nitrate and algal DOM in this study were added at the high end of a range that would occur in source water, and in full-scale case studies the effects may not be as pronounced. Figures 40 and 41 present the effect of matrix and UV dose for different processes on NDMA formation and compare processes at given UV dose and matrix on NDMA formation.

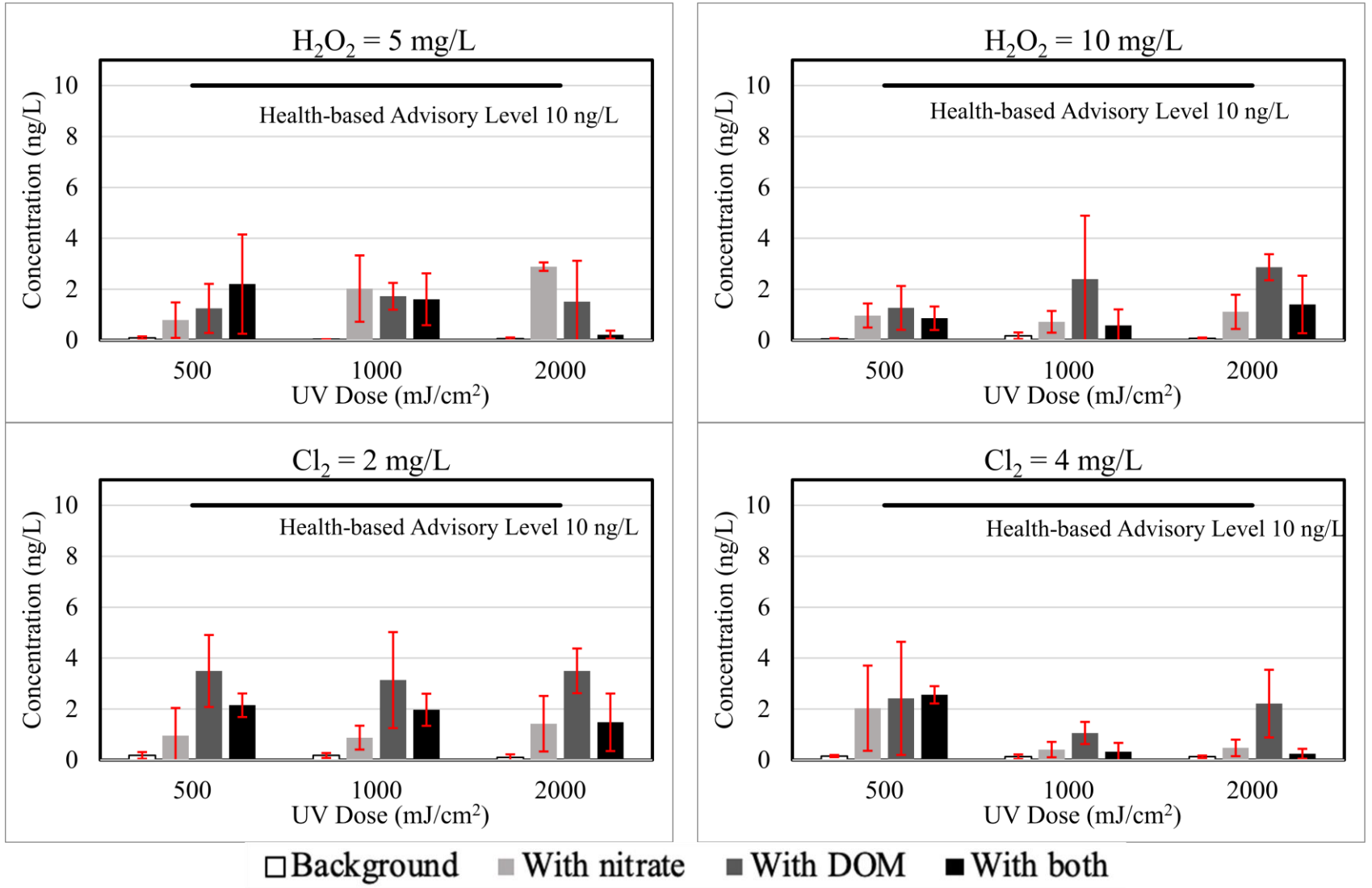

Figure 40. Effect of matrix and UV dose for different processes on NDMA formation.
Figure shows the average of three separate experiments with the error bars showing standard deviation.

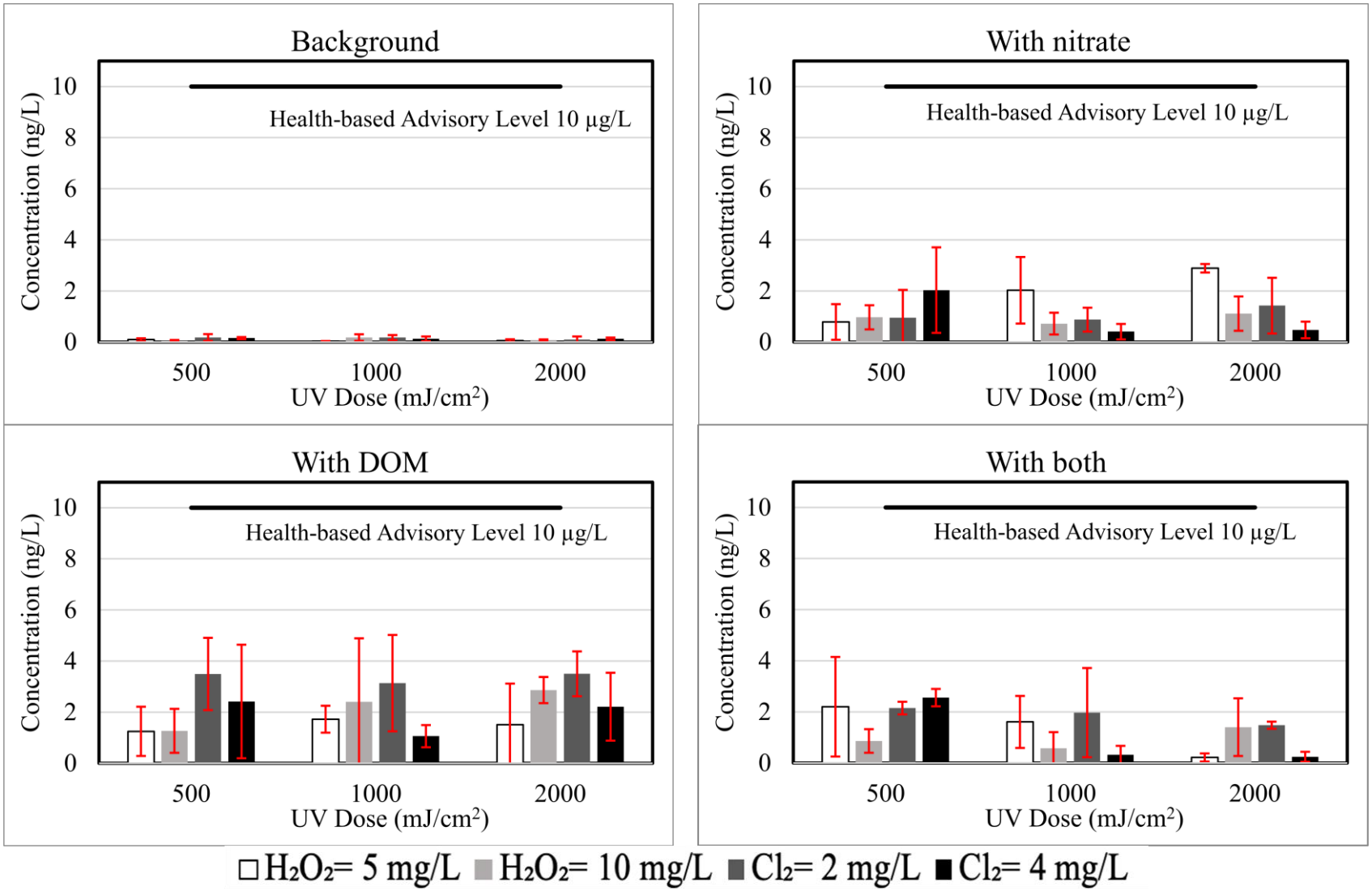

Figure 41. Effect of processes at a given UV dose and matrix on NDMA formation.
Figure shows the average of three separate experiments with the error bars showing standard deviation.

Conclusions

Both UV/H_2O_2 and UV/Cl_2 processes were effective in oxidizing the three tested microcystin variants (LR, RR, and YR). Microcystins have a fast reaction with chlorine, and direct chlorination reaction had a major contribution to the overall decomposition of the toxins, in particular MC-LR.

Algal DOM addition had a different inhibitory effect for each toxin because of their relative reactivity with radicals. Nitrate enhanced the degradation of MCs due to additional hydroxyl radicals produces under low-wavelength UV emitted by MP UV lamps. However, with both DOM and nitrate in the water matrix, the effect of DOM as a radical scavenger was higher than the impact of nitrate as a source of radicals.

While PP2A assays were inconclusive due to matrix interferences that could not be separated, the LC/MS results suggest that the Adda group responsible for toxicity is susceptible and likely the products would not exhibit the toxicity of the parent compound.

Based on the results for THMs, chloroform was increased with AOM presence in hydrogen peroxide processes and was suppressed by nitrate. AOM also increased the formation of bromodichloromethane in UV/H_2O_2 process. The maximum TTHM concentration was 46.26 µg/L belonging to the background matrix that was treated using Cl_2 = 4 mg/L and UV = 2000 mJ/cm^2. None of the samples exceeded the MCL.

Three HAAs were detectable in the treated samples, including tribromoacetic acid, chlorodibromoacetic acid, and monochloroacetic acid. HAAs results showed that tribromoacetic acid formation was higher in samples containing nitrate (not statistically significant). No correlation was observed between the type of process or the level of treatment and HAA formation. Monochloroacetic acid was formed during UV/H_2O_2 processes, which was significantly suppressed by the addition of nitrate and algal DOM to the background matrix. The maximum THAAs was 127.8 µg/L belonging to matrix containing 20 mg/L NO_3 treated by H_2O_2 5 mg/L under UV = 1000 mJ/cm^2. However, in most of the samples THAAs concentration was less than MCL (60 mg/L).

Findings on NDMA demonstrated that both nitrate and algal DOM increased the formation of NDMA. However, the concentration of nitrate and DOM were on the high end of an environmentally relevant range. Additionally, the level of NDMA was less than 10 ng/L at all treatment conditions and in all background matrices.

Other Outcomes

Training: The project provided hands-on experience for one PhD student and one undergraduate student, enabling them to process concepts learned in class and preparing them for future employment. The graduate student received training on advanced oxidation processes and toxicity assays in preparation for highly technical work in the field of water treatment. She received a post-doctoral position that specifically relied on the training she gained performing

the work on this study. The undergraduate student was trained in basic laboratory research skills, providing her a strong basis for future graduate work. She has since been accepted into our MS program.

Information transfer: The results of the study were presented at two national conferences and were scheduled to be presented at another conference in North Carolina (NC WRRI) meeting, but the last talk was cancelled due to coronavirus concerns. Below are the listings of the presentations:

1. Barancheshme, F., and Keen, O. (2019) Algal toxins in drinking water: UV/Cl_2 and UV/H_2O_2 advanced oxidation processes as treatment method. ACS Annual Meeting, San Diego, CA.
2. Barancheshme, F., and Keen, O. (2020) Treatment of algal organic matter in drinking water with UV/Cl_2 and UV/H_2O_2 advanced oxidation: Assessment of disinfection byproduct formation. IUVA Americas Meeting, Orlando, FL.
3. Barancheshme, F., and Keen, O. (2020) Treatment of algal organic matter in drinking water with UV/Cl_2 and UV/H_2O_2 advanced oxidation. NC WRRI Conference, Raleigh, NC. (conference cancelled due to Covid-19)

A paper manuscript is currently in development based on the work performed in this study.

References Cited

1. Loftin, K. A.; Graham, J. L.; Hilborn, E. D.; Lehmann, S. C.; Meyer, M. T.; Dietze, J. E.; Griffith, C. B., Cyanotoxins in inland lakes of the United States: Occurrence and potential recreational health risks in the EPA National Lakes Assessment 2007. *Harmful Algae* **2016,** *56*, 77-90.
2. Loftin, K. A.; Clark, J. M.; Journey, C. A.; Kolpin, D. W.; Van Metre, P. C.; Carlisle, D.; Bradley, P. M., Spatial and temporal variation in microcystin occurrence in wadeable streams in the southeastern United States. *Environmental Toxicology and Chemistry* **2016,** *35* (9), 2281-2287.
3. Beaver, J. R.; Manis, E. E.; Loftin, K. A.; Graham, J. L.; Pollard, A. I.; Mitchell, R. M., Land use patterns, ecoregion, and microcystin relationships in U.S. lakes and reservoirs: A preliminary evaluation. *Harmful Algae* **2014,** *36*, 57-62.
4. Graham, J. L.; Loftin, K. A.; Kamman, N., Monitoring recreational freshwaters. *Lakeline* **2009,** *29*, 18-24.
5. Rosenfeldt, E. J. In *UV advanced oxidation for treatment of taste and odor and algal toxins*, Ohio AWWA Annual Conference Research Workshop, 2011.
6. Drikas, M.; Chow, C. W. K.; House, J.; Burch, M. D., USING COAGULATION, FLOCCULATION AND SETTLING REMOVE TOXIC cyanobacteria. *Journal (American Water Works Association)* **2001,** *93* (2), 100-111.
7. Karner, D. A.; Standridge, J. H.; Harrington, G. W.; Barnum, R. P., Microcystin algal toxins IN SOURCE AND FINISHED DRINKING WATER. *Journal (American Water Works Association)* **2001,** *93* (8), 72-81.
8. Hall, T.; Hart, J.; Croll, B.; Gregory, R., Laboratory-Scale Investigations of Algal Toxin Removal by Water Treatment. *Water and Environment Journal* **2000,** *14* (2), 143-149.
9. Rositano, J.; Newcombe, G.; Nicholson, B.; Sztajnbok, P., Ozonation of nom and algal toxins in four treated waters. *Water Research* **2001,** *35* (1), 23-32.
10. Orr, P. T.; Jones, G. J.; Hamilton, G. R., Removal of saxitoxins from drinking water by granular activated carbon, ozone and hydrogen peroxide—implications for compliance with the Australian drinking water guidelines. *Water Research* **2004,** *38* (20), 4455-4461.
11. Rodríguez, E.; Onstad, G. D.; Kull, T. P. J.; Metcalf, J. S.; Acero, J. L.; von Gunten, U., Oxidative elimination of cyanotoxins: Comparison of ozone, chlorine, chlorine dioxide and permanganate. *Water Research* **2007,** *41* (15), 3381-3393.
12. Merel, S.; Clément, M.; Thomas, O., State of the art on cyanotoxins in water and their behaviour towards chlorine. *Toxicon* **2010,** *55* (4), 677-691.
13. de la Cruz, A. A.; Hiskia, A.; Kaloudis, T.; Chernoff, N.; Hill, D.; Antoniou, M. G.; He, X.; Loftin, K.; O'Shea, K.; Zhao, C.; Pelaez, M.; Han, C.; Lynch, T. J.; Dionysiou, D. D., A review on cylindrospermopsin: the global occurrence, detection, toxicity and degradation of a potent cyanotoxin. *Environmental Science: Processes & Impacts* **2013,** *15* (11), 1979-2003.
14. Cook, D.; Newcombe, G., COMPARISON AND MODELING OF THE ADSORPTION OF TWO MICROCYSTIN ANALOGUES ONTO POWDERED ACTIVATED CARBON. *Environmental Technology* **2008,** *29* (5), 525-534.
15. Song, W.; De la Cruz, A. A.; Rein, K.; O'Shea, K. E., Ultrasonically induced degradation of microcystin-LR and -RR: Identification of products, effect of pH, formation and destruction of peroxides. *Environmental Science & Technology* **2006,** *20* (12), 3941-3946.

16. Song, W.; Xu, T.; Cooper, W. J.; Dionysiou, D. D.; De la Cruz, A. A.; O'Shea, K. E., Radiolysis studies on the destruction of microcystin-LR in aqueous solution by hydroxyl radicals. *Environ Sci Technol* **2009,** *43* (5), 1487-92.
17. Senogles, P. J.; Scott, J. A.; Shaw, G.; Stratton, H., Photocatalytic Degradation of the Cyanotoxin Cylindrospermopsin, using Titanium Dioxide and UV Irradiation. *Water Research* **2001,** *35* (5), 1245-1255.
18. Shephard, G. S.; Stockenström, S.; de Villiers, D.; Engelbrecht, W. J.; Wessels, G. F. S., Degradation of microcystin toxins in a falling film photocatalytic reactor with immobilized titanium dioxide catalyst. *Water Research* **2002,** *36* (1), 140-146.
19. Afzal, A.; Oppenländer, T.; Bolton, J. R.; El-Din, M. G., Anatoxin-a degradation by Advanced Oxidation Processes: Vacuum-UV at 172 nm, photolysis using medium pressure UV and UV/H2O2. *Water Research* **2010,** *44* (1), 278-286.
20. He, X.; Pelaez, M.; Westrick, J. A.; O'Shea, K. E.; Hiskia, A.; Triantis, T.; Kaloudis, T.; Stefan, M. I.; de la Cruz, A. A.; Dionysiou, D. D., Efficient removal of microcystin-LR by UV-C/H2O2 in synthetic and natural water samples. *Water Research* **2012,** *46* (5), 1501-1510.
21. Watts, M. J.; Rosenfeldt, E. J.; Linden, K. G., Comparative OH radical oxidation using UV-Cl2 and UV-H2O2 processes. *Journal of Water Supply: Research and Technology - Aqua* **2007,** *56* (8), 469-477.
22. Sichel, C.; Garcia, C.; Andre, K., Feasibility studies: UV/chlorine advanced oxidation treatment for the removal of emerging contaminants. *Water Research* **2011,** *45* (19), 6371-6380.
23. Wang, D.; Bolton, J. R.; Hofmann, R., Medium pressure UV combined with chlorine advanced oxidation for trichloroethylene destruction in a model water. *Water Research* **2012,** *46* (15), 4677-4686.
24. Watts, M. J.; Hofmann, R.; Rosenfeldt, E. J., Low-pressure UV/Cl 2 for advanced oxidation of taste and odor. *Journal: American Water Works Association* **2012,** *104* (1).
25. Zhou, S.; Shao, Y.; Gao, N.; Zhu, S.; Li, L.; Deng, J.; Zhu, M., Removal of Microcystis aeruginosa by potassium ferrate (VI): Impacts on cells integrity, intracellular organic matter release and disinfection by-products formation. *Chemical Engineering Journal* **2014,** *251*, 304-309.
26. Gad, A. A. M.; El-Tawel, S., Effect of pre-oxidation by chlorine/permanganate on surface water characteristics and algal toxins. *Desalination and Water Treatment* **2016,** *57* (38), 17922-17934.
27. Fang, J.; Ma, J.; Yang, X.; Shang, C., Formation of carbonaceous and nitrogenous disinfection by-products from the chlorination of Microcystis aeruginosa. *Water Research* **2010,** *44* (6), 1934-1940.
28. Dotson, A. D.; Keen, V. S.; Metz, D.; Linden, K. G., UV/H2O2 treatment of drinking water increases post-chlorination DBP formation. *Water Research* **2010,** *44* (12), 3703-3713.
29. Beaulieu, M.; Pick, F.; Gregory-Eaves, I., Nutrients and water temperature are significant predictors of cyanobacterial biomass in a 1147 lakes data set. *Limnology and Oceanography* **2013,** *58* (5), 1736-1746.
30. Gobler, C. J.; Burkholder, J. M.; Davis, T. W.; Harke, M. J.; Johengen, T.; Stow, C. A.; Van de Waal, D. B., The dual role of nitrogen supply in controlling the growth and toxicity of cyanobacterial blooms. *Harmful Algae* **2016,** *54*, 87-97.
31. Wang, D. Z.; Hsieh, D., Effects of nitrate and phosphate on growth and C2 toxin productivity of Alexandrium tamarense CI01 in culture. *Marine pollution bulletin* **2002,** *45* (1-12), 286-9.

32. Mack, J.; Bolton, J. R., Photochemistry of nitrite and nitrate in aqueous solution: a review. *Journal of Photochemistry and Photobiology A: Chemistry* **1999,** *128* (1–3), 1-13.
33. Keen, O. S.; Love, N. G.; Linden, K. G., The role of effluent nitrate in trace organic chemical oxidation during UV disinfection. *Water Res* **2012,** *46* (16), 5224-34.
34. Deng, Y.; Wu, M.; Zhang, H.; Zheng, L.; Acosta, Y.; Hsu, T. D., Addressing harmful algal blooms (HABs) impacts with ferrate(VI): Simultaneous removal of algal cells and toxins for drinking water treatment. *Chemosphere* **2017,** *186*, 757-761.
35. Adams, J. L.; Tipping, E.; Feuchtmayr, H.; Carter, H. T.; Keenan, P., The contribution of algae to freshwater dissolved organic matter: implications for UV spectroscopic analysis. *Inland Waters* **2018,** *8* (1), 10-21.
36. Lee, D.; Kwon, M.; Ahn, Y.; Jung, Y.; Nam, S.-N.; Choi, I.-h.; Kang, J.-W., Characteristics of intracellular algogenic organic matter and its reactivity with hydroxyl radicals. *Water Research* **2018,** *144*, 13-25.
37. Graham, J. L.; Loftin, K. A.; Meyer, M. T.; Ziegler, A. C., Cyanotoxin Mixtures and Taste-and-Odor Compounds in Cyanobacterial Blooms from the Midwestern United States. *Environmental Science & Technology* **2010,** *44* (19), 7361-7368.
38. Kristiana, I.; Lethorn, A.; Joll, C.; Heitz, A., To add or not to add: The use of quenching agents for the analysis of disinfection by-products in water samples. *Water Research* **2014,** *59*, 90-98.
39. Keen, O.; Dotson, A.; Linden, K., Evaluation of Hydrogen Peroxide Chemical Quenching Agents following an Advanced Oxidation Process. *Journal of Environmental Engineering* **2013,** *139* (1), 137-140.
40. Klassen, N. V.; Marchington, D.; McGowan, H. C. E., H2O2 Determination by the I3- Method and by KMnO4 Titration. *Analytical Chemistry* **1994,** *66* (18), 2921-2925.
41. Walker, H. W., *Harmful Algae Blooms in Drinking Water: Removal of Cyanobacterial Cells and Toxins*. CRC Press: 2014.
42. Bolton, J.; Linden, K., Standardization of Methods for Fluence (UV Dose) Determination in Bench-Scale UV Experiments. *Journal of Environmental Engineering* **2003,** *129* (3), 209-215.
43. Mountfort, D. O.; Holland, P.; Sprosen, J., Method for detecting classes of microcystins by combination of protein phosphatase inhibition assay and ELISA: comparison with LC-MS. *Toxicon* **2005,** *45* (2), 199-206.
44. Summers; S., R.; Hooper; M., S.; Shukairy; M., H.; Solarik; G.; Owen; D., *Assessing DBP yield : uniform formation conditions*. American Water Works Association: Denver, CO, ETATS-UNIS, 1996; Vol. 88.
45. Liu, X.; Wei, X.; Zheng, W.; Jiang, S.; Templeton, M. R.; He, G.; Qu, W., An optimized analytical method for the simultaneous detection of iodoform, iodoacetic acid, and other trihalomethanes and haloacetic acids in drinking water. *PLoS One* **2013,** *8* (4), e60858-e60858.
46. Zhao, Y.-Y.; Boyd, J.; Hrudey, S. E.; Li, X.-F., Characterization of New Nitrosamines in Drinking Water Using Liquid Chromatography Tandem Mass Spectrometry. *Environmental Science & Technology* **2006,** *40* (24), 7636-7641.
47. Environmental Protection Agency, Six-year review 3 technical support document for nitrosamines. **2016,** *EPA 810-R-16-009*.
48. Charrois, J. W. A.; Arend, M. W.; Froese, K. L.; Hrudey, S. E., Detecting N-Nitrosamines in Drinking Water at Nanogram per Liter Levels Using Ammonia Positive Chemical Ionization. *Environmental Science & Technology* **2004,** *38* (18), 4835-4841.

49. Acero, J. L.; Rodriguez, E.; Meriluoto, J., Kinetics of reactions between chlorine and the cyanobacterial toxins microcystins. *Water Res* **2005,** *39* (8), 1628-38.
50. Ho, L.; Onstad, G.; Gunten, U. v.; Rinck-Pfeiffer, S.; Craig, K.; Newcombe, G., Differences in the chlorine reactivity of four microcystin analogues. *Water Research* **2006,** *40* (6), 1200-1209.
51. He, X.; de la Cruz, A. A.; Hiskia, A.; Kaloudis, T.; O'Shea, K.; Dionysiou, D. D., Destruction of microcystins (cyanotoxins) by UV-254 nm-based direct photolysis and advanced oxidation processes (AOPs): Influence of variable amino acids on the degradation kinetics and reaction mechanisms. *Water Research* **2015,** *74*, 227-238.
52. Westerhoff, P.; Aiken, G.; Amy, G.; Debroux, J., Relationships between the structure of natural organic matter and its reactivity towards molecular ozone and hydroxyl radicals. *Water Research* **1999,** *33* (10), 2265-2276.
53. Carmichael, W. W.; Boyer, G. L., Health impacts from cyanobacteria harmful algae blooms: Implications for the North American Great Lakes. *Harmful Algae* **2016,** *54*, 194-212.
54. Carmichael, W. W.; An, J., Using an enzyme linked immunosorbent assay (ELISA) and a protein phosphatase inhibition assay (PPIA) for the detection of microcystins and nodularins. *Natural toxins* **1999,** *7* (6), 377-85.
55. Sedan, D.; Laguens, M.; Copparoni, G.; Aranda, J. O.; Giannuzzi, L.; Marra, C. A.; Andrinolo, D., Hepatic and intestine alterations in mice after prolonged exposure to low oral doses of Microcystin-LR. *Toxicon* **2015,** *104*, 26-33.
56. Sohn, J.; Amy, G.; Yoon, Y., Bromide Ion Incorporation Into Brominated Disinfection By-Products. *Water Air Soil Pollut* **2006,** *174* (1), 265-277.
57. Tan, J.; Allard, S.; Gruchlik, Y.; McDonald, S.; Joll, C. A.; Heitz, A., Impact of bromide on halogen incorporation into organic moieties in chlorinated drinking water treatment and distribution systems. *Science of The Total Environment* **2016,** *541*, 1572-1580.
58. Egeberg, P. K.; Eikenes, M.; Gjessing, E. T., Organic nitrogen distribution in NOM size classes. *Environment International* **1999,** *25* (2), 225-236.